

# Deep Image Matting: A Comprehensive Survey

Jizhizi Li, Jing Zhang, *Member, IEEE*, Dacheng Tao, *Fellow, IEEE*

**Abstract**—Image matting refers to extracting precise alpha matte from natural images, and it plays a critical role in various downstream applications, such as image editing. Despite being an ill-posed problem, traditional methods have been trying to solve it for decades. The emergence of deep learning has revolutionized the field of image matting and given birth to multiple new techniques, including automatic, interactive, and referring image matting. This paper presents a comprehensive review of recent advancements in image matting in the era of deep learning. We focus on two fundamental sub-tasks: auxiliary input-based image matting, which involves user-defined input to predict the alpha matte, and automatic image matting, which generates results without any manual intervention. We systematically review the existing methods for these two tasks according to their task settings and network structures and provide a summary of their advantages and disadvantages. Furthermore, we introduce the commonly used image matting datasets and evaluate the performance of representative matting methods both quantitatively and qualitatively. Finally, we discuss relevant applications of image matting and highlight existing challenges and potential opportunities for future research. We also maintain a public repository to track the rapid development of deep image matting at <https://github.com/JizhiziLi/matting-survey>.

**Index Terms**—Image Matting, Computer Vision, Deep Learning, Survey.



## 1 INTRODUCTION

IMAGE matting is a fundamental computer vision problem that involves extracting the precise alpha matte of foreground objects from arbitrary natural images. This technique is particularly suitable for categories that have very fine details, such as humans [1], [2], [3], animals [4], and plants [5]. Image matting serves as an essential procedure for various downstream tasks, including promotional advertising in practical e-commerce platforms, image editing for daily life entertainment, background replacing for on-line video conferences, and metaverse applications such as virtual reality and game industries.

Image matting, initially referred to as the *travelling-matte problem* in the film-making industry [6], [7], has been a subject of research for several decades. However, due to the ill-posed nature of the problem, traditional methods have relied on various auxiliary user inputs to alleviate the challenge. These inputs include trimap [8], [9], [10], [11] and scribble [12], [13], [14], [15], or specific conditions such as blue-screen [6], [16]. Previous methods for image matting can be divided into two main streams. The first stream [17] employs color sampling to estimate the unknown pixels from neighbouring ones, while the latter stream defines an affinity matrix [13] to propagate the known foreground and background to the transition area. Both of the two streams rely on low-level color or structure features, which limit their ability to distinguish foreground details from complex backgrounds, resulting in sensitivity to the size of the unknown area and fuzzy boundaries [18], [19].

In recent years, deep learning has emerged as a new approach to solving various computer vision problems including image matting [20]. Researchers have designed new solutions based on deep convolutional neural networks (CNNs) that are capable of learning discriminative features [1], [21]. These approaches typically follow the

conventional settings of using auxiliary user input to add a constraint to the ill-posed problem, which can include trimap [22], [23], [24], [25], [26], scribble [27], background image [28], coarse map [21], [29], or even text description [30]. Some methods concatenate the image and auxiliary inputs and pass them through a single-stage network [22], [24], [31], [32] with or without an auxiliary module, while others leverage a multi-stream structure for task-aware optimization [33], [34]. Although these approaches have produced results with better details than traditional solutions, they still require a significant amount of manual effort to provide auxiliary inputs. To address this limitation, more flexible auxiliary input options have been explored, such as user-click [35], [36], [37] or text description [30]. Furthermore, the success of transformer [38] and Vision Transformer [39], [40], [41] has also led to the introduction of these structures in image matting [30], [42], [43].

In contrast to the above methods, automatic image matting methods aim to predict the foreground of an image without requiring any user intervention [1], [44]. These methods typically predict specific salient foreground objects, which are implicitly defined by the training dataset, *e.g.*, human [1], [2], [45], [46], [47], animal [4], or composite foregrounds [48], [49], [50]. Recently, AIM [5] categorizes the foreground objects in nature images into three kinds, *i.e.*, salient opaque, salient transparent, and non-salient, and processes them through a single model. As per the network structure, automatic matting methods can be divided into three groups: one-stage network with global guidance [51], sequential segmentation and matting network [1], [2], and parallel multi-task network [4], [5] to model subtasks explicitly. Recently, some methods have also introduced transformer structures [52], [53] into automatic image matting [3]. These methods use the self-attention mechanism to capture long-range dependencies and context information, which can improve the accuracy of the predictions.

To facilitate the training and evaluation of deep learning-based methods, many datasets have been proposed over the

Jizhizi Li, Jing Zhang, and Dacheng Tao are with the School of Computer Science, Faculty of Engineering, The University of Sydney, Australia (e-mail: jili8515@uni.sydney.edu.au; jing.zhang1@sydney.edu.au; dacheng.tao@gmail.com)

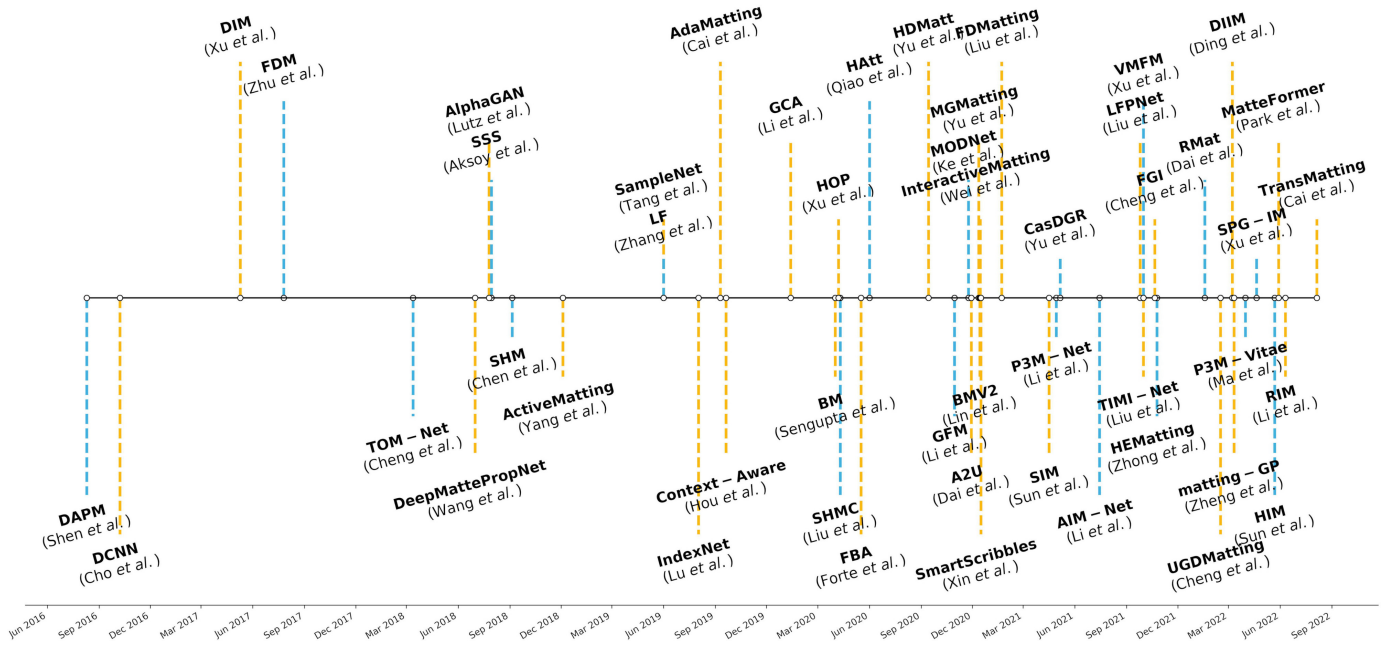


Fig. 1. The timeline presents a historical overview of deep learning-based image matting methods. The blue lines indicate the auxiliary input-based matting methods, while the yellow lines indicate the automatic matting methods.

years. The first such dataset was proposed by alphamatt [54], containing 27 images and a benchmark website. Since then, numerous datasets have been proposed by researchers, containing different content categories, image resolutions, composition styles, and annotation strategies [1], [2], [4], [5], [22], [29], [46], [47], [48], [49]. Due to the laborious and costly labelling process, many early works [22], [48], [49] either use chroma keying to extract foregrounds and alpha blending [55] to compose synthetic images with backgrounds from MS COCO [56] and Pascal VOC [57] or adopt existing matting methods close-form [12], and KNN [58] to compute matte labels. Although these early datasets provide valuable training data and facilitate the development of deep learning-based methods, the composition artifacts and limited resolution could mislead trained models and result in poor generalization abilities on natural images [4], [46]. Recently, some researchers have proposed high-resolution natural image datasets along with manually labeled alpha mattes to resolve these issues [4], [5], [29], [46]. Furthermore, privacy-preserving dataset [47] has also been established to address ethical issues in portrait image matting.

In this article, we present a comprehensive review of recent advancements in image matting achieved through the use of deep learning techniques. We discuss two broad categories of methods: auxiliary input-based matting and automatic matting. We also cover the different datasets used for training and testing these methods, evaluate their performance, and discuss the potential applications and future work. We have reviewed 69 papers from top-tier conferences and journals and compiled a timeline of the developments in deep learning-based image matting in Figure 1, highlighting the growing intensity of research in this area. To keep pace with the fast development, we have

established a public repository<sup>1</sup> that provides an up-to-date record of recent advancements. In summary, this review aims to provide researchers and practitioners in this field with a comprehensive understanding of the current state-of-the-art techniques, their performance, related applications, and potential avenues for future work.

### 1.1 Contributions of this Survey

Compared with prior matting surveys that predominantly focus on traditional methods [59], [60], [61], [62], [63], this paper provides a comprehensive review of image matting methods, with a specific emphasis on those utilizing deep learning techniques, making it unique and important in both scope and depth. The contributions of this survey can be summarized as follows:

- We make the first attempt to provide a comprehensive summary and literature review of deep learning-based image matting methods.
- We examine the progress made in deep image matting from several perspectives, including input and output forms, network structures, and benchmark datasets.
- We offer a fair and comprehensive evaluation of the performance of deep image matting methods, while also analyzing their model complexity.
- We discuss promising applications of image matting and highlight the challenges and potential opportunities for further research.

### 1.2 Relationship to Other Surveys

In order to provide a comprehensive understanding of the research landscape and contextualize our analysis of

1. <https://github.com/JizhiziLi/matting-survey>

deep image matting methods, we suggest consulting several excellent previous surveys that focus on image matting [61], [62], [63], [64] and related research topics, e.g., video matting [60], [65], image composition [66], semantic segmentation [67], [68], [69], [70], [71], and salient object detection [72], [73], [74]. Previous surveys on image matting have primarily focused on traditional solutions, examining aspects such as methodologies [60], [62], and pre-processing strategies [64]. These methods have been categorized as sampling-based [17], affinity-based [9], [12], [75], or a combination of the two [8], [14], [76]. Other works have explored downstream applications of image matting, such as video matting [15], [77], [78], environment matting [79], [80], [81], shadow matting [82], [83], composition [84], and harmonization [85]. While some surveys on relevant research topics have provided comprehensive analyses of methodologies and datasets [65], [67], [72], they have not investigated image matting in depth. In contrast, this paper surveys large amounts of relevant image matting methods, with a particular focus on those based on deep learning.

### 1.3 Organization

The remainder of this paper is structured as follows. In Section 2, we present some preliminary background information regarding the problem statement, taxonomy, and traditional solutions. Section 3 reviews auxiliary input-based matting models from the perspective of various input forms. Section 4 discusses automatic matting methods that use either sequential or parallel structures. Section 5 provides an overview of both composite and natural matting datasets. In Section 6, we conduct a performance evaluation and analysis of representative matting methods on several benchmark datasets. Subsequently, in Section 7, we present the relevant applications of deep image matting, followed by a discussion of the challenges and opportunities in Section 8. Finally, we conclude the review in Section 9.

## 2 PRELIMINARY

### 2.1 Problem Statement

Image matting, which refers to the precise extraction of the soft matte from foreground objects in arbitrary images, has been extensively studied for several decades. The concept was initially introduced by Beyer [6] in the 1960s and later mathematically formalized by Porter and Duff [7] in the 1980s. Subsequently, researchers have referred to this problem as *pulling matte*, *matte creation* [86], or *chromakey* [16]. The problem has been studied in conjunction with the problem of *digital composition* [87], [88], [89].

$$I_i = \alpha_i F_i + (1 - \alpha_i) B_i, \quad \alpha_i \in [0, 1]. \quad (1)$$

The image matting process can be described mathematically using Eq. (1), where  $I$  represents the input image,  $F$  represents the foreground image, and  $B$  represents the background image. In this equation, the color of the  $i$ th pixel is approximated as a convex combination of the corresponding foreground and background colors. The opacity of the pixel in the foreground is denoted by  $\alpha_i$ , which ranges from 0 to 1. If  $\alpha_i$  equals 1, the pixel is classified as a *pure foreground* or *definite foreground*. Conversely, if  $\alpha_i$  equals 0, it

is classified as a *pure background* or *definite background*. Pixels with opacity values ranging from 0 to 1 are known as the *unknown region* or *transition area*. Since  $I$  is a three-channel RGB image, image matting is defined by three equations and seven unknown variables, resulting in a heavily ill-posed problem that requires in-depth research study.

### 2.2 Taxonomy

In this section, we discuss deep learning-based matting methods using a taxonomy that encompasses the input modality, matting target, and methodology. Table 1 summarizes the reviewed papers, ordered by their release dates.

#### 2.2.1 Input Modality

Matting methods adopt different input modalities that suit both automatic and auxiliary-based methodologies. For methods that require auxiliary information to constrain the solution space, the input modalities can be further categorized into various types, including RGB image with trimap [24], [31], [32], [90], RGB image with background images [28], [91], RGB image with coarse maps [21], [29], RGB image with user click [36], [37], RGB image with flexible inputs [92], and RGB image with text descriptions [30]. Among these input modalities, the *trimap* is the most commonly used, which is a three-class map that indicates the pure foreground, pure background, and unknown region [60]. Each type of auxiliary input provides varying degrees of aid in easing the burden of the ill-posed matting problem. On the other hand, for automatic methods [2], [4], [44], [93] designed for automatic industrial applications, the input modality is a single RGB image that can be either a composite one or a natural one.

#### 2.2.2 Matting Target

In general, there are no restrictions on the types of foreground objects that can be processed as matting targets. However, the (generalization) ability of deep learning-based image matting methods is limited by the foreground types available in the training dataset. Several studies have focused on human (portrait) matting, as portraits are a prevalent subject in the matting task [1], [3], [28], [45], [46]. Other researchers have explored foreground types that have meticulous details, such as animals [4], or transparent objects [93], [94]. In [5], the matting targets are categorized into three groups: salient opaque foregrounds, salient transparent foregrounds, and non-salient foregrounds, which represent a typical taxonomy of matting targets.

#### 2.2.3 Methodology

The taxonomy of matting methodologies can be approached from two perspectives, namely auxiliary input-based methods and automatic methods. With regard to the former, the methodologies can be classified into three categories. Firstly, a single one-stage CNN is used to directly map the concatenation of the input image and the auxiliary input to the alpha matte [22], [23], [25]. Secondly, a one-stage CNN is used with modules carefully designed to make use of the rich features from the auxiliary input through the side branch [31], [37], [95]. Thirdly, parallel two- or multi-stream structures are utilized to decompose the matting

task into explicit sub-tasks [28], [34], [96]. Some of these methodologies require an additional refiner to further refine the predicted alpha matte [22], [91]. More details about these methodologies will be discussed in Section 3.

For automatic matting methods, there are also three main methodologies. The first is a one-stage structure, which can optionally include a global module [48], [51] as guidance to predict the matte directly from a single input. The second is a sequential two-step structure, where an intermediate segmentation mask or trimap is generated first, and then combined with the initial input to produce the final alpha matte [1], [2], [44], [45]. The third methodology is a parallel two- or multi-stream structure, which decomposes the matting task into several sub-tasks such as foreground and background or global semantic mask [49] and local details [4], [5], [47]. Some of these methodologies also require a refiner to refine the alpha matte [93]. More details about these methodologies will be discussed in Section 4.

### 2.3 Traditional Solutions

Prior to the advent of deep learning, researchers have made significant efforts to tackle image matting problems using traditional solutions. In the initial stages, the input image usually has a blue, green, or constant-color background, which is known as *blue screen matting* [16], [112]. It can reduce the difficulty of the problem and make it more tractable. Furthermore, *triangular matting* is derived [8], [113] to assist in generating the ground-truth alpha mattes. To expand to natural images with complex backgrounds or even videos, additional information was utilized to constrain the problem, including trimap [8], [9], [58], scribble [12], [13], [76], flash or non-flash image pairs [114], camera arrays [115], and multiple synchronized video streams [116].

The traditional solutions for matting can be categorized into three types. Firstly, color sampling-based methods rely on the strong correlation between nearby image pixels to sample from known foreground or background colors and apply them to unknown pixels [17], [18], [117]. Secondly, affinity-based methods calculate the affinity matrix to characterize the similarity between neighboring pixels and propagate alpha values from known areas to unknown areas accordingly [9], [13], [15], [62], [113], [117], [118]. Thirdly, the combination of both sampling-based and affinity-based methods is adopted for optimization to achieve more robust solutions [8], [14], [119], [120]. Although these methods have shown significant improvements in predicting results through comprehensive design, their representation abilities are limited by low-level color or structure features, and they struggle to distinguish foreground details from complex natural backgrounds. Additionally, since most of these methods require manually labeled auxiliary inputs, the results are usually very sensitive to the size of the unknown region and fuzzy boundaries.

## 3 AUXILIARY INPUT-BASED IMAGE MATTING

In this section, we provide a comprehensive review of the different types of auxiliary input-based matting models that utilize various input modalities such as trimap, scribble, background, coarse map, user interactive click, and text

descriptions. An example of the input image and different auxiliary inputs is shown in Figure 2. Additionally, we summarize the architectures of the auxiliary input-based matting methods in Figure 3, which can be categorized into three types: 1) a one-stage model that processes the concatenation of the input image and auxiliary input; 2) a one-stage model that processes the concatenation of the input image and auxiliary input, and leverages the information of the auxiliary input with an outsider module; and 3) two- or multi-stream model that processes input image, auxiliary input, or their combination separately, and then passes through a fusion model to generate the final output. We discuss the details of these methods, along with their advantages, challenges, and comparisons with each other in the following part.

### 3.1 Trimap-based Auxiliary Input

After transitioning from blue screen matting to natural image matting, researchers began using the auxiliary input of a *trimap* [18], [121]. It is a three-class map that indicates the definite foreground, definite background, and unknown region, as shown in Figure 2. A trimap is typically defined by the user or generated by off-the-shelf segmentation models [122] with dilation operations [123]. Although it significantly reduces the difficulty of the problem, it requires manual effort, which remains a challenge to achieve a good trade-off. With the advent of deep learning, advanced solutions utilize one of the three architectures shown in Figure 3.

#### 3.1.1 One-stage Architecture

The initial attempts of deep learning-based approaches to natural image matting with trimap input typically adopt a simple one-stage architecture. For example, DIM [22] first solves the problem by concatenating the image and trimap as input and processing it through a fully convolutional network [124] with a U-net skip connection [125] based on VGG-16 [126] to predict the output. FBA [25] utilizes a similar structure based on ResNet-50 [127] as the backbone but predicts seven channels instead of one, including one for the alpha matte, three for the foreground, and three for the background. AlphaGAN [90] and MatteFormer [42] adopt a similar one-stage architecture but with a generative adversarial network (GAN) [128] and Swin Transformer [40], respectively. SmartScribbles [27] oversamples the image into superpixels and rectangular regions and automatically selects the most informative ones for users to draw scribble, then propagates it through a two-phase propagation. TransMatting [94] presents a trimap-guided transformer block [40] between the ResNet-34 encoder and decoder to maintain the contexture of transparent objects.

#### 3.1.2 One-stage Architecture with Outsider Module

While the one-stage architecture used in some deep learning-based methods is simple and intuitive, it has limitations in exploiting auxiliary information. To address this issue, some methods [23], [24], [31], [95], [108] have introduced outsider modules that specifically process auxiliary information or the concatenation of auxiliary and input. For example, DMPN [31] uses a module to extract low-level features and then applies a matte propagation module as

TABLE 1

Summary of image matting methods organized according to the year of publication, the publication venue, input modality, automaticity, matting target, architecture, train set, and test set. Please note that the list of papers is chronologically ordered.

Year	Method	Pub.	Modality	Automatic	Target	Architecture	Train Set	Test Set
2016	DAPM [1]	ECCV	RGB	✓	human	Sequential two-step CNN	DAPM-2k [1]	DAPM-2k [1]
	DCNN [21]	ECCV	RGB-Coarse		object	One-stage CNN	AlphaMatting [54]	AlphaMatting [54]
2017	DIM [22]	CVPR	RGB-Trimap		object	One-stage CNN+Refine	DIM-481 [22]	DIM-481 [22]
	FDM [44]	MM	RGB	✓	human	Sequential two-step CNN	DAPM-2k [1]	DAPM-2k [1]
2018	TOM-Net [93]	CVPR	RGB	✓	transparent	Sequential two-step CNN + Refine	TOM-876 [93]	TOM-876 [93]
	DMPN [31]	IJCAI	RGB-Trimap		object	One-stage CNN	DMPN-46 [31]	DMPN-46 [31]
	AlphaGAN [90]	BMVC	RGB-Trimap		object	One-stage GAN	DIM-481 [22]	DIM-481 [22]
	SSS [97]	TOG	RGB	✓	object	Sequential two-stage structure	COCO-Stuff [98]	DIM-481 [22]
	SHM [2]	MM	RGB	✓	human	Sequential two-step CNN	SHM-35k [2]	SHM-35k [2]
	ActiveMatting [35]	NeurIPS	RGB-Click		object	One-stage RNN	DAPM-2k [1]	DAPM-2k [1]
2019	LF [49]	CVPR	RGB	✓	object	Sequential two-stage CNN	DIM-481 [22], LF-257 [49]	DIM-481 [22], LF-257 [49]
	SampleNet [33]	CVPR	RGB-Trimap		object	Parallel three-stream CNN	DIM-481 [22]	DIM-481 [22]
	IndexNet [24]	ICCV	RGB-Trimap		object	One-stage CNN	DIM-481 [22]	DIM-481 [22]
	AdaMatting [34]	ICCV	RGB-Trimap		object	Parallel two-stream CNN + Refine	DIM-481 [22]	DIM-481 [22]
	Context-Aware [32]	ICCV	RGB-Trimap		object	Two-stream CNN	DIM-481 [22]	DIM-481 [22]
2020	GCA [23]	AAAI	RGB-Trimap		object	One-stage CNN	DIM-481 [22]	DIM-481 [22]
	BM [28]	CVPR	RGB-Background		human	Parallel four-stream CNN	DIM-481 [22], BM-Video [28]	DIM-481 [22], BM-Video [28]
	HOP [99]	arXiv	RGB-Trimap		object	Parallel two-stream CNN	DIM-481 [22]	DIM-481 [22]
	SHMC [45]	CVPR	RGB	✓	human	Sequential two-stage CNN	SHMC-10k [45]	SHMC-10k [45]
	FBA [25]	arXiv	RGB-Trimap		object	One-stage CNN	DIM-481 [22]	DIM-481 [22]
	HATt [48]	CVPR	RGB	✓	object	One-stage CNN	DIM-481 [22], HATT-646 [48]	DIM-481 [22], HATT-646 [48]
	HDMatt [96]	AAAI	RGB-Trimap		object	Parallel two-stream CNN	DIM-481 [22]	DIM-481 [22], DAPM-2k [1]
	GFM [4]	IJCV	RGB	✓	human, animal	Parallel two-stream CNN	AM-2k [4], PM-10k [4]	AM-2k [4], PM-10k [4]
	MODNet [46]	AAAI	RGB	✓	human	Parallel two-stream CNN	SPD [100], PPM-3000 [46]	PPM-100 [46]
	AZU [101]	CVPR	RGB-Trimap		object	One-stage CNN	DIM-481 [22], HATT-646 [48]	DIM-481 [22], HATT-646 [48]
	MGMatting [29]	CVPR	RGB-Coarse		human	One-stage CNN	DIM-481 [22]	DIM-481 [22]
	InteractiveMatting [36]	CVPR	RGB-Click		object	Parallel two-stream CNN	DIM-481 [22]	DIM-481 [22]
	SmartScribbles [27]	TOMM	RGB-Scribble		object	One-stage CNN	DAPM [1], DIM-481 [22]	DAPM [1], DIM-481 [22]
	BMV2 [91]	CVPR	RGB-Background		human	One-stage CNN + Refiner	DIM-481 [22], HATT-646 [48], VM-24 [91], PhotoMatte13k [91]	PhotoMatte85 [91]
2021	FDMatting [102]	WACV	RGB-Trimap		object	Two-stream CNN	DIM-481 [22]	DIM-481 [22]
	SIM [95]	CVPR	RGB-Trimap		object	One-stage CNN	SIM [95]	SIM [95], DIM-481 [22]
	P3M-Net [47]	MM	RGB	✓	human	Parallel two-stream CNN	P3M-10k [47]	P3M-10k [47]
	CasDGR [51]	ICCV	RGB	✓	object	Multi-scale multi-stage CNN	DIM-481 [22]	DIM-481 [22]
	AIM-Net [5]	IJCAI	RGB	✓	object	Parallel two-stream CNN	DUTS [103], AM-2k [4], DIM-481 [22], HATT-646 [48]	AIM-500 [5]
	LFPNet [104]	MM	RGB-Trimap		object	Parallel two-stream CNN	DIM-481 [22]	DIM-481 [22]
	VMFM [105]	ICCV	RGB	✓	human-object	Sequential two-stage CNN	DIM-481 [22], HATT-646 [48], LFM40k [105], UFM75k [105]	DIM-481 [22], LFM40k [105]
	TIMI-Net [26]	ICCV	RGB-Trimap		object	Parallel three-stream CNN	DIM-481 [22], HATT-646 [48], Human-2k [26]	DIM-481 [22], HATT-646 [48], Human-2k [26]
FGI [92]	BMVC	RGB-Flexible		object	One-stage CNN	DIM-481 [22]	DIM-481 [22]	
HEMatting [106]	BMVC	RGB	✓	object	Sequential two-stage CNN	DIM-481 [22]	DIM-481 [22]	
2022	RMat [43]	CVPR	RGB-Trimap		object	Parallel two-stream CNN/Transformer	DIM-481 [22]	DIM-481 [22], AIM-500 [5]
	DIIM [37]	TIP	RGB-Click		object	One-stage CNN	DIM-481 [22], FIO [37]	DIM-481 [22]
	UGDMatting [107]	TIP	RGB-Flexible		human	Parallel two-stream CNN	UGD-12k [107], HATT-646 [48]	UGD-12k [107], HATT-646 [48]
	matting-GP [108]	TNNLS	RGB-Trimap		object	One-stage CNN	DIM-481 [22], real-set2 [108]	DIM-481 [22], real-set2 [108]
	P3M-ViTAE [3]	IJCV	RGB	✓	human	Parallel two-stream CNN/Transformer	P3M-10k [47]	P3M-10k [47]
	SPG-IM [109]	MM	RGB	✓	object	Sequential two-stage CNN	DIM-481 [22], Multi-Object-1K [109], Human-2k [110], HATT-646 [48]	DIM-481 [22], Multi-Object-1K [109], Human-2k [110], HATT-646 [48]
	HIM [111]	CVPR	RGB	✓	human	Sequential two-stage CNN	HIM2k [111]	HIM2k [111], RWP636 [29]
	MatteFormer [42]	CVPR	RGB-Trimap		object	One-stage CNN	DIM-481 [22]	DIM-481 [22]
	RIM [30]	CVPR	RGB-Language		object	Parallel two-stream CNN/Transformer	RefMatte [30]	RefMatte [30]
TransMatting [94]	ECCV	RGB-Trimap		transparent	One-stage CNN/Transformer	Trans-460 [94]	Trans-460 [94]	

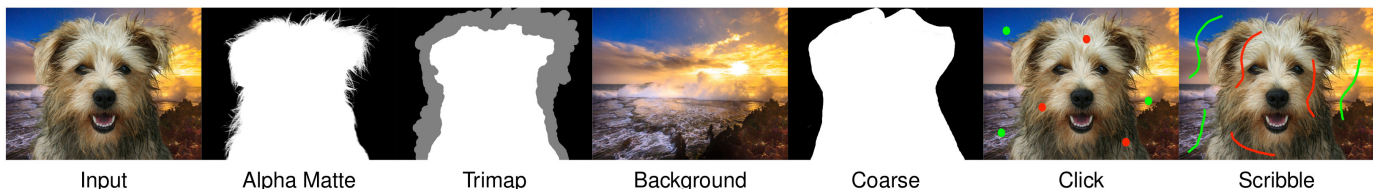


Fig. 2. Illustration of a typical input image along with its alpha matte and various auxiliary inputs such as trimap, background, coarse map, user clicks, scribbles, and a text description that are commonly employed in auxiliary input-based image matting methods. The text description of the image can be the cute smiling brown dog in the middle of the image. In the click and scribble inputs, red lines or dots denote the pure foreground, while green lines or dots indicate the pure background. The foreground and background images used in this illustration are sourced from the AM-2k and BG-20k datasets [4]. We suggest enlarging the image for a more detailed view.

a refiner. IndexNet [24] proposes a module that dynamically predicts indices for individual local regions, which are then used to preserve details through downsampling and upsampling stages. GCA [23] designs a module to directly propagate high-level opacity information globally based on learned low-level affinity. SIM [95] uses a patch-based classifier to incorporate semantic classification of matting regions by extending the conventional trimap to a semantic one. Matting-GP [108] provides a Gaussian process to encapsulate the expressive power of deep architecture and reduce computation complexity.

### 3.1.3 Multi-stream Architecture

Various methods in recent years [26], [32], [33], [34], [43], [96], [99], [102], [104] have acknowledged the advantages of processing diverse levels of multi-task information through multi-stream encoders and subsequently fusing it via a shared decoder. For instance, SampleNet [33] estimates same-level foreground and background via a two-stream sample-selection process before predicting the opacity of the whole image. TIMI-Net [26], on the other hand, employs a three-branch encoder to supplement the neglected coordination between RGB space and trimap space, along with

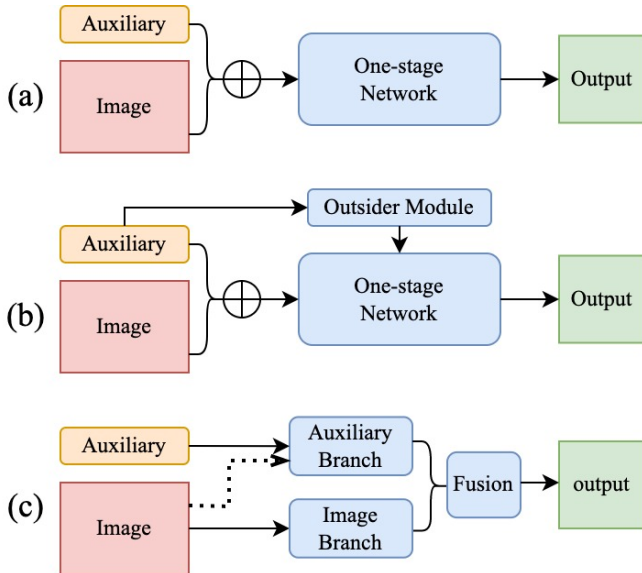


Fig. 3. The architectures of the auxiliary input-based matting methods can be categorized into one of three types: (a) a one-stage model; (b) a one-stage model with an outsider module that processes auxiliary information; or (c) a two- or multi-stream model that processes the auxiliary input and the input image in separated streams.

additional interactions. Other approaches strive to leverage global context information and local details simultaneously for sub-task aware propagation before the fusion network, such as the adapted trimap and alpha in AdaMatting [34], the foreground and alpha in Context-aware [32], the image appearance and alpha opacity in HOP [99], the image patch with trimap and context patch with trimap in HDMatt [96], the semantic path containing an image with trimap and a textural path containing an image with noisy trimap in FDMatting [102], the downsampled images’ context and surrounding image patches’ features in LFPNet [104], and the transformer-based context and convolutional-based details in RMat [43]. These solutions lead to a deeper understanding of different information levels and a learnable fusion model for better collaboration.

### 3.2 Pre-defined Auxiliary Input

In addition to the commonly used trimap, some methods employ pre-defined images, such as backgrounds [28], [91], or coarse maps [21], [29] as auxiliary inputs.

#### 3.2.1 Background-based Matting Model

Due to the time-consuming nature of obtaining trimaps, some researchers have proposed alternative methods for obtaining auxiliary inputs. For instance, BM [28] and BMV2 [91] require an additional photo of the background, which is captured by the user beforehand, as shown in Figure 2. However, these methods are often limited to human matting targets. In BM [28], a soft segmentation is first computed and then passed through a network [129] to estimate the foreground and alpha matte with an adversarial loss. On the other hand, BMV2 [91] provides a base network to compute a low-resolution result, which is then refined by a second network that operates at high-resolution on patches.

#### 3.2.2 Coarse-based Matting Model

Although background-based matting provides good results, it has limitations in certain scenarios and requires some level of foresight. Consequently, some researchers have explored the use of coarse segmentation maps [21], [29] as inputs instead, as shown in Figure 2. For instance, DCNN [21] produces auxiliary coarse maps using CF [12] and KNN [58], which are then combined with the original image and fed into a one-stage CNN network. A2U [101] proposes to leverage second-order features to formulate an affinity-aware upsampling block, which replaces the normal block in a ResNet34-based one-stage CNN structure. MGMatting [29] adopts an encoder-decoder architecture with the image and coarse map as inputs, using a self-guidance mechanism to progressively refine uncertain regions.

### 3.3 User-interactive Auxiliary Input

To address the limitations of pre-defined auxiliary inputs, researchers have explored the use of user-interactive auxiliary inputs. These methods [35], [36], [37], [92], [107] allow users to interactively provide auxiliary inputs that can dynamically refine the results.

#### 3.3.1 Click-based Matting Model

Several works [35], [36], [37] incorporate user click, as shown in Figure 2, as an auxiliary input. For example, ActiveMatting [35] proposes a recurrent reinforcement learning framework [130], [131] that involves human interaction through clicks. InteractiveMatting [36] uses a two-decoder network to take RGB image and click as input and refines the result using an uncertainty-guided local refinement module. DIIM [37] transforms user clicks into a distance map, concatenates it with the original image, and passes it through an encoder-decoder network and a full-resolution extraction module to predict the alpha matte.

#### 3.3.2 Flexible User Input-based Matting Model

Other approaches [27], [92], [107] in the field choose more flexible inputs as auxiliary signals, such as scribble. For instance, FGI [92] employs an encoder-decoder structure that gradually reduces the area of the uncertain region in the auxiliary input, thereby improving the prediction of the final alpha matte. UGDMatting [107] uses a double-encoder and double-decoder to extract image features, propagate user interaction data, and generate foreground and background before a fusion model predicts the final result. SmartScribbles [27] guides users to draw only a few scribbles to achieve high-quality matting results.

### 3.4 Text-based Auxiliary Input

In recent research, there has been a trend to explore the integration of other input modalities with the input image to enable a more controllable matting procedure. For example, text descriptions have been used to provide flexible auxiliary information. One representative work is RIM [30], which utilizes a CLIP-based [132] two-branch encoder-decoder framework to extract text-driven semantic features from the original image while preserving local matting details. Additionally, RIM has established RefMatte, a large-scale benchmark dataset with massive amounts of paired

image and text descriptions, which will be discussed in detail in Section 5.

### 3.5 Summary

Data-driven methods that utilize auxiliary inputs have become prevalent in the era of deep learning, as they can provide more precise results than fully automatic approaches. In recent years, various forms of auxiliary inputs have been explored to provide different benefits, such as trimap, background, coarse map, click map, scribble, and even text description. With the development of this field, the form of auxiliary input has become increasingly flexible and less time-consuming, allowing for more interactive and intuitive matting procedures.

As previously discussed, the methodologies for auxiliary input-based image matting can be broadly classified into three types. The first type is the one-stage network, which directly predicts the alpha matte from the input image and the auxiliary input. The second type is the one-stage network with a specially designed external module that processes the auxiliary input before fusing it with the image features to obtain the final alpha matte. The third type is the multi-stream model, which processes the input and the auxiliary input at different levels before fusing them to generate the final output. Each of these methods improves upon the previous one by utilizing the features from the auxiliary input and performing subtask-aware global-local collaboration.

Despite their success, these methods may have two potential limitations. Firstly, they still require varying degrees of manual effort, which may not be feasible for automatic industrial applications. Additionally, certain inputs such as background images may require foresight that is not available in many practical scenarios. Secondly, most of these methods exhibit high sensitivity to specific auxiliary inputs, such as the size of the transition area in trimap, the accuracy of the coarse map, the density of the clicks, and the shape of strokes, making the development of robust methods a significant challenge.

## 4 AUTOMATIC IMAGE MATTING

To overcome the limitations of auxiliary input-based matting methods and render them applicable to real-world industrial settings, scholars have put forward automatic matting methods that predict the alpha matte from the input image without relying on any auxiliary input. In this section, we review these methods, focusing on their architectures as illustrated in Figure 4, as well as their matting targets.

### 4.1 One-stage Matting Model

Several studies, including HATT [48], MODNet [46], and CasDGR [51], propose a one-stage model with an optional guidance module, as illustrated in Figure 4(a). HATT employs a ResNeXt [133] network that utilizes skip-connections, along with a global guidance module that incorporates channel-wise and spatial-wise attention mechanisms, to predict alpha matte directly from the input image. Similarly, MODNet employs a MobileNetV2 [134] CNN as

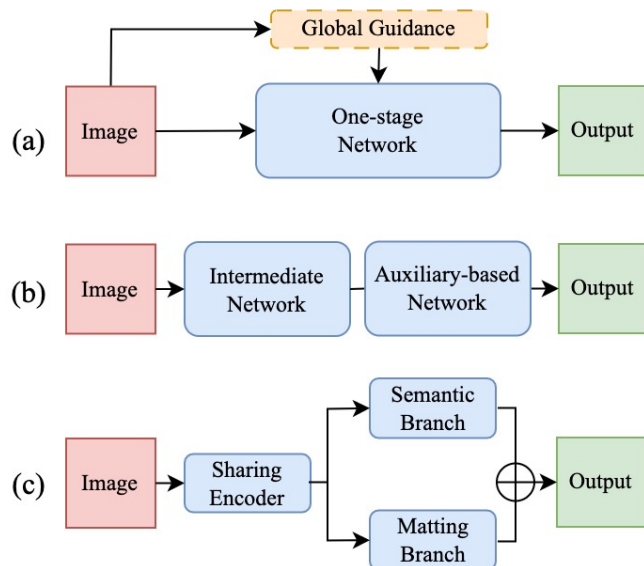


Fig. 4. The architectures of the automatic matting methods can be classified into one of three types: (a) a one-stage model with an optional global guidance module; (b) a sequential two-step model that predicts intermediate and final outputs; or (c) an encoder-sharing network with two or more separate decoders.

its backbone network and incorporates several convolutional layers as its global guidance. CasDGR utilizes graph neural networks (GNNs) [135], [136] to optimize its one-stage network, producing the output from coarse to fine.

### 4.2 Sequential Matting Model

An alternative solution to automatic matting is a sequential two-step architecture, depicted in Figure 4(b). In this method, the first network is utilized to generate an intermediate representation, such as a trimap, a coarse map, or a combination of the foreground, background, and unknown regions. Its goal is to alleviate the difficulty of the problem by simplifying the second stage, and transforming it into a straightforward auxiliary input-based matting problem. This methodology is widely employed and has been adopted in numerous studies.

#### 4.2.1 Trimap as the Intermediate

The most straightforward intermediate representation is the trimap. DAPM [1] and SHM [2] predict it through the intermediate network, *e.g.*, FCN-8s [124] in DAPM and PSPNet-50 [137] in SHM. These two methods are both tailored for human matting.

#### 4.2.2 Coarse Map as the Intermediate

Another commonly used intermediate representation is the coarse map, which can be generated using an off-the-shelf segmentation network such as MaskRCNN [122] as in HIM [111], or a carefully designed network as in FDM [44], SHMC [45], and SPG-IM [109]. Specifically, FDM [44] uses densely connected blocks [138] with dilated convolution [139] as the intermediate network, while SHMC [45] utilizes an encoder-decoder CNN with skip connections. SPG-IM [109] adopts a ResNet-50 [127] captioning encoder,

a transformer-based [38] text decoder, and an Atrous Spatial Pyramid Pooling (ASPP) [139] based encoder-decoder. As for the auxiliary-based network in the second stage, HIM [111] utilizes the one provided in MGMatting [29], while FDM [44] devises a feature block with guided filter [140]. SHMC [45] chooses an encoder-decoder with skip-connections, and SPG-IM [109] leverages a ResNet-50 encoder-decoder.

#### 4.2.3 Other Intermediate

Some other works use different types of intermediate representations, such as foreground and background [49], unknown regions [106], depth maps and heatmaps [105], albedo maps, shading maps, and specular maps [93]. In LF [49], the foreground and background probability maps are obtained using a DenseNet-201 [138]-based encoder and then fed into an FCN fusion network for prediction. HEMatting [106] employs an OctConv [141]-based encoder-decoder network to produce 3-channel classification logits and another one for the final output. VMFM [105] generates a depth map through DenseDepth [142], a human segmentation map through Mask-RCNN [122], and a human-object paired heatmap following the work [143] as the intermediate representations. It then produces alpha matte using a dual network and a complementary learning module to estimate the deviation probability map for predicting the final output. TOM-Net [93] uses a mirror-link CNN [144] to predict an albedo map, a shading map, and a specular map, which are then concatenated with the input image and passed through a residual network for obtaining the final result. SSS [97] extracts high-level semantic features from DeepLab-ResNet-101 [139] and proposes a graph structure to predict soft labels using the Laplacian matrix from embedding texture and color features.

### 4.3 Encoder Sharing Model

Although the previous two architectures offer an intuitive design for automatic matting, recent works [3], [4], [5], [47] explicitly decompose the task into several sub-tasks, learn mutual features through sharing an encoder, and formulate each sub-task as a separate decoder branch, as shown in Figure 4(c). Each decoder output should be supervised by the relevant ground truth to ensure that each sub-task is optimized properly. Finally, a hard fusion mechanism is used to produce the final result from the outputs of all the decoders. It typically has two decoders for global semantic segmentation and local matting, respectively. In the semantic decoder, the output can be foreground and background masks [4], or trimap [3], [4], [5], [47]. GFM [4] uses DenseNet-121 [138], ResNet-34 [127], or ResNet-101 as the backbone of the shared encoder, a pyramid pooling module (PPM) [137], [145] in the global decoder and a bridge block [146] in the local decoder. AIM-Net [5] devises a spatial attention module to guide the matting decoder by leveraging the learned semantic features from the semantic decoder to focus on extracting details within the transition area. P3M-Net [47] designs a tripartite-feature integration, a shallow bipartite-feature integration, and a deep bipartite-feature integration to model interactions among the shared encoder and two decoders. Specifically, P3M-ViTAE [3]

adopts the ViTAE transformer [41], [52] as the shared encoder to better represent the long-range global context and local detail features.

### 4.4 Matting Target

Automatic matting methods, which are designed without any auxiliary input, are prone to training data bias. As a result, most of these methods are limited to specific matting targets, such as human [46], animal [4], and transparent objects [93]. In this regard, we provide a detailed discussion and comparison of the existing methods. Several methods, such as DAPM [1], SHM [2], CasDGR [51], FDM [44], SHMC [45], and MODNet [46], focus on the most prevalent matting target, *i.e.*, *human*. Some methods, including VMFM [105] and SPG-IM [109], focus on human-object interaction. HIM [111] is designed for predicting the alpha matte of human instances. P3M-Net [47] and P3M-ViTAE [3] produce an alpha matte for privacy-preserving human images. GFM [4] is designed to process both human and animal images, while TOM-Net [93] is trained to learn the opacity map of transparent objects. Other methods, such as HATT [48], LF [49], and HEMatting [106], work on normal types of objects. AIM-Net [5] further divides them into salient opaque foregrounds, salient transparent/meticulous foregrounds, and non-salient foregrounds, with a carefully designed generalized trimap for each type.

### 4.5 Summary

Automatic methods have been developed to reduce the need for time-consuming manual labelling of auxiliary inputs. These methods can be categorized into three types of architectures: 1) a one-stage network with an optional global guidance module, 2) a sequential stage-wise network that predicts intermediate representation and produces the alpha matte sequentially, and 3) an encoder-sharing networks with separate decoders that generate sub-tasks' outputs before a final fusion block. Various intermediate representations have been investigated, including trimap, coarse map, foreground, background, and unknown regions, depth map, heatmap, shading map, and others. However, due to the high demand for training data, these methods are prone to biases towards specific matting targets, such as humans, human-object interaction, animals, transparent objects, salient objects, and non-salient objects.

Despite the advantages of automatic matting methods for practical industrial applications, there are still some limitations that need to be addressed. Firstly, without auxiliary inputs, these methods tend to extract all salient or centralized foregrounds, which can result in less controllable outcomes that require significant manual effort to improve. Secondly, due to the bias towards training data, it is important to consider how to generalize these methods to new categories and unseen data. Lastly, to be applied in industrial settings, it is crucial to develop models that are lightweight and computationally efficient, capable of operating in real-time.

## 5 IMAGE MATTING DATASETS

Deep learning-based methods rely heavily on high-quality training and testing datasets [148], and this holds true for



TABLE 2

Summary of image matting datasets, categorized as the synthetic image-based benchmark, natural image-based benchmark, and test sets. The datasets are ordered based on their release date and are described in terms of publication venue, source modality, label type, naturalness, matting target, resolution, annotation method, number of training and test samples, and availability. It should be noted that the size of the datasets is calculated based on the number of distinguished foregrounds, except for TOM [93] and RefMatte [30], which have pre-defined composite rules.

Method	Pub.	Modality	Label	Natural	Target	Resolution	Annotation	#Train	#Test	Public
DIM-481 [22]	CVPR'17	Image, Video frame	alpha		object	1,298 × 1,083	Manually	431	50	✓
TOM [93]	CVPR'18	3D model	alpha, refractive flow		transparent	-	POV-Ray [147]	178,000	876	✓
LF-257 [49]	CVPR'19	Image	alpha		human	553 × 756	Manually	228	29	✓
HATT-646 [48]	CVPR'20	Image	alpha		object	1,573 × 1,731	Manually	596	50	✓
PhotoMatte13k [91]	CVPR'20	Image	alpha		human	-	Manually	13,665	-	✓
SIM [95]	CVPR'21	Image	alpha		object	2,194 × 1,950	Manually	348	50	✓
Human-2k [26]	ICCV'21	Image	alpha		human	2,112 × 2,075	Manually	2,000	100	✓
Trans-460 [94]	ECCV'22	Image	alpha		transparent	3,766 × 3,820	Manually	410	50	✓
HIM2k [111]	CVPR'22	Image	alpha		human	1,823 × 1,424	Manually	1500	500	✓
RefMatte [30]	CVPR'23	Image	alpha, language		object	1,543 × 1,162	Manually	45,000	2,500	✓
AlphaMatting [54]	CVPR'09	Image	alpha	✓	object	3,056 × 2,340	Manually	27	8	✓
DAPM-2k [1]	ECCV'16	Image	alpha	✓	human	600 × 800	KNN [58], CF [12]	1700	300	✓
SHM-35k [2]	MM'18	Image	alpha	✓	human	-	Manually	52,511	1,400	✓
SHMC-10k [45]	CVPR'20	Image	alpha, coarse map	✓	human	-	Manually	9,324	125	✓
P3M-10k [47]	MM'21	Image	alpha	✓	human	1,349 × 1,321	Manually	9,421	1,000	✓
AM-2k [4]	IJCV'22	Image	alpha	✓	animal	1,471 × 1,195	Manually	1,800	200	✓
Multi-Object-1K [109]	MM'22	Image	alpha	✓	human-object	-	Manually	1000	200	✓
UGD-12k [107]	TIP'22	Image	alpha	✓	human	356 × 317	Manually	12,066	700	✓
PhotoMatte85 [91]	CVPR'20	Image	alpha		human	2,304 × 3,456	Manually	-	85	✓
AIM-500 [5]	IJCAI'21	Image	alpha	✓	object	1,397 × 1,260	Manually	-	500	✓
RWP-636 [29]	CVPR'21	Image	alpha, detail map	✓	human	1,038 × 1,327	Manually	-	636	✓
PPM-100 [46]	AAAI'22	Image	alpha	✓	human	2,997 × 2,875	Manually	-	100	✓

the task of image matting as well. This section provides a comprehensive review of image matting datasets, spanning from traditional methods to contemporary ones. We categorize the datasets into two types: synthetic image-based datasets and natural image-based datasets. Table 2 provides a summary of these datasets, and we discuss their details in the following subsections.

## 5.1 Synthetic Matting Datasets

Because it is time-consuming to manually label meticulous alpha mattes of foregrounds, many matting datasets [22], [30], [48], [49], [95] consist of synthetic images created by extracting the foregrounds from simple or plain backgrounds and compositing them with complex backgrounds using alpha blending [12]. DCNN [21] first introduces a synthetic dataset by compositing 27 foregrounds from AlphaMatting [54] with numerous backgrounds. DIM [22] introduces 481 foregrounds, with 27 from AlphaMatting [54], some frames from video datasets [149], and images from plain backgrounds. The alpha mattes are manually generated by Photoshop [150], and the backgrounds used in composition are from MS COCO [56] and Pascal VOC [151]. TOM [93] renders multiple 3D models using POV-ray [147] to create large amounts of synthetic transparent datasets. LF [49] contains 257 human images from the internet with carefully annotated alpha mattes. HATT [48] provides 646 distinct foregrounds of multiple categories to improve the diversity of the matting datasets. PhotoMatte [91] has 13k synthetic high-resolution human foregrounds, but only 85 test images are publicly available. SIM [95] collects 398 images from 20 classes that are widely used in matting scenarios and annotates the alpha mattes using Photoshop. Human-2k [26] is a high-resolution human dataset containing 2,100 synthetic images. RIM [30] establishes RefMatte containing 13,187 foregrounds from public synthetic matting datasets, along with their category labels, to form 45,000 training images and 2,500 test images with backgrounds from BG-20k [4]. RefMatte also provides text description labels to

help develop models for referring image matting. Please note that the number of synthetic datasets shown in Table 2 is calculated on a per-foreground basis, and each foreground is usually blended with 20 to 100 backgrounds. Trans-460 [94] introduces 460 transparent object foregrounds to facilitate the study of transparent matting. HIM2k [111] collects 2,000 human images with alpha mattes, of which 360 are natural images and the rest are synthetic. Please note that since TOM [93] and RefMatte [30] have predefined explicit composite rules for generating the training datasets, we report the actual amount of training data directly.

Although using synthetic datasets to train deep learning models for image matting enjoys the benefits of providing large amounts of training data with various complex backgrounds, it also results in a domain gap between composite images and natural images, due to the *composition artifacts* that arise from discrepancies between the foregrounds and backgrounds [4], [152], [153]. Numerous works have observed such phenomena [4], [26], [27], [29], [30], [93], [107], [109], [111], and some have focused on reducing these discrepancies and improving the generalization ability on real-world natural images [4], [28], [32], [43], [46]. For example, Context-Aware [32] applies re-JPEGging and Gaussian blur as data augmentation following the work [154], [155]. GFM [4] proposes a composition route called RSSN to address issues such as resolution, sharpness, noise, and illumination discrepancies. They also build a large-scale high-resolution dataset BG-20k that contains diverse background images. BM [28] describes a self-supervised scheme to learn from unlabelled real data and a discriminator to improve the result. MODNet [46] fine-tunes the model on unlabeled real data by using consistency between sub-objectives to reduce the domain gap. RMat [43] employs strong data augmentations, such as linear pixel-wise augmentation, non-linear pixel-wise augmentation, and region-wise augmentation, to mitigate the domain gap.

## 5.2 Natural Matting Datasets

To enhance the generalization capability of matting models to real-world images, some researchers have established natural image matting datasets, encompassing a diverse range of categories such as humans [47], animals [4], and objects [54]. Table 2 provides a summary of these datasets, presenting their source modality, type of labels, matting target, average resolution, annotation method, as well as the number of training and testing images, and availability.

AlphaMatting [54] captures high-quality ground truth mattes in a restricted studio environment using triangulation [16] and augments the data [156] to yield a total of 35 high-resolution images. It also offers a complete online benchmark system with carefully designed error measures, which provides great value for trimap-based methods, especially in the traditional solutions era. However, with the emergence of data-driven deep learning methods, large-scale matting datasets have become essential. Therefore, DAPM [1] collects 2,000 human portrait images with ground truth labels generated by off-the-shelf methods KNN [58] and CF [12]. Subsequently, to enhance image resolution and label accuracy, researchers have established large-scale datasets with manually annotated alpha mattes focusing on humans [2], [45], [47], [107], animals [4], and human-objects [109]. However, many of these datasets are not public due to privacy or licensing issues, which impedes future research in the community. P3M-10k [47] addresses this issue by providing the first large-scale privacy-preserving portrait matting dataset with carefully annotated alpha mattes of 10,421 human images in various backgrounds. AM-2k [4] is the first animal matting dataset that contains 2,000 images from 20 categories. UGD [107] also provides a large number of public portrait images, although the resolution is somewhat limited for the matting task.

In addition to the aforementioned benchmark datasets, there exist several test-only real-world matting datasets that aim to facilitate the evaluation of matting models' generalization ability. For instance, AIM-500 [5] is the first natural image matting dataset that comprises 500 high-resolution images of different categories, along with alpha mattes labeled by professionals. RWP-636 [29] introduces 636 real-world portrait images, where additional detail map labels are provided to indicate the most challenging detail regions. PPM-100 [46] is another publicly available real-world human dataset, consisting of 100 images.

## 5.3 Summary

High-quality datasets and accurate labels are essential for the success of deep learning-based image matting. However, creating such datasets is a significant challenge. To tackle this issue, researchers have established several valuable datasets that are publicly available. These datasets can be broadly classified into two categories: synthetic and composite datasets, each with its strengths and limitations.

Synthetic datasets require relatively little manual effort and can generate a large number of training images by easily composing each foreground with many various backgrounds. However, these synthetic images can exhibit composition artifacts that may introduce a significant domain gap when compared to real-world images. On the other

hand, natural matting datasets do not suffer from such issues and the trained models can easily adapt to real-world images. However, they may be limited to specific matting targets and smaller scales due to the difficulty of accurately extracting alpha mattes from images in the wild. Additionally, the manual labelling process for generating ground truth alpha mattes may introduce errors or noise. Thus, developing a scalable approach for generating high-quality and large-scale image matting datasets remains a significant challenge.

## 6 PERFORMANCE BENCHMARKING

In this section, we provide a comprehensive evaluation of representative matting methods. A thorough examination of the training objectives (refer to Table 3) and evaluation metrics is presented. Additionally, a fair and rigorous benchmarking of both auxiliary-based and automatic models is carried out (refer to Table 4), followed by an in-depth analysis of the results.

TABLE 3

Summary of losses used in deep learning-based matting methods.

	Auxiliary	Automatic
$\mathcal{L}_{alpha}$	[22], [31], [90], [43], [24], [34], [32], [23], [28], [37], [25] [96], [29], [36], [91], [102], [95], [104], [26], [92], [33], [99], [107], [42], [94]	[1], [44], [2], [49], [111], [4], [46], [47], [51], [109], [105], [106], [3], [5], [45]
$\mathcal{L}_{comp}$	[22], [31], [90], [33], [24], [28], [25], [96], [29], [91], [104], [92], [43], [42], [94]	[44], [2], [45], [4], [105], [47], [51], [5], [46], [3], [111]
$\mathcal{L}_{mse}$	[21], [32], [36], [37], [95], [91], [107], [108], [35]	[93], [49], [48], [46]
$\mathcal{L}_{ce}$	[34], [27], [95], [37], [107]	[93], [2], [49], [4], [47], [5], [106], [3]
$\mathcal{L}_{lap}$	[32], [25], [29], [43], [42], [94]	[4], [47], [5], [3], [111]
$\mathcal{L}_{grad}$	[33], [25], [95], [92], [43], [107]	[51], [106]
$\mathcal{L}_{adv}$	[90]	[48], [105]
$\mathcal{L}_{multi}$	[34]	-
$\mathcal{L}_{ssim}$	-	[48]

### 6.1 Training Objectives

To enable the effective training of deep learning-based matting models, researchers have developed various loss functions. In this section, we outline the definitions of the most commonly used loss functions and present a summary of them in Table 3, with a focus on their application in both auxiliary input-based models and automatic models.

**Alpha loss** The alpha loss function, denoted as  $\mathcal{L}_{alpha}$ , is calculated as the absolute difference between the ground truth alpha matte,  $\alpha_g$ , and the predicted alpha matte,  $\alpha_p$ , on a per-pixel basis. To ensure the differentiability of the loss, a small value  $\varepsilon$  is typically added [22], as demonstrated in Eq. (2). Here,  $i$  denotes the index of the pixel and  $\varepsilon$  is set to  $10^{-6}$  for computational stability. The weight for each pixel,  $W_\alpha^i \in [0, 1]$ , is constantly set to 1 for automatic matting models, and for auxiliary-based methods, it is set to 1 in transition areas and 0 in the foreground and background regions. Some studies [1] have also utilized different weights for each pixel when calculating the loss.

$$\mathcal{L}_{alpha} = \frac{\sum_i \sqrt{((\alpha_p^i - \alpha_g^i) \times W_\alpha^i)^2 + \varepsilon^2}}{\sum_i W_\alpha^i}. \quad (2)$$

**Composition loss** The composition loss function, denoted as  $\mathcal{L}_{comp}$ , is computed as the absolute difference between the ground truth RGB values,  $C_g^i$ , and the predicted RGB values,  $C_p^i$ , which are obtained via alpha blending [12]. Similar to the alpha loss function, a small value  $\varepsilon$  is added for differentiability, and the weight  $W_c^i \in [0, 1]$  is set following the same procedure as previously mentioned.

$$\mathcal{L}_{comp} = \frac{\sum_i \sqrt{((C_p^i - C_g^i) \times W_c^i)^2 + \varepsilon^2}}{\sum_i W_c^i}. \quad (3)$$

**MSE loss** The MSE loss function, which stands for mean squared error, computes the average squared difference between the ground truth alpha matte,  $\alpha_g$ , and the predicted alpha matte,  $\alpha_p$ , as shown in Eq. (4). The weight  $W_\alpha^i \in [0, 1]$  has the same meaning as previously mentioned. Some studies [35] have used root mean square error instead, while others [32] have computed MSE between high-level features instead of the final output. There are other works [36], [37], [49], [92], [102], [107] have opted to use the alpha loss for the transition area, and the MSE loss for the foreground and background regions, or vice versa, to better leverage the benefits of each loss function.

$$\mathcal{L}_{mse} = \frac{\sum_i ((\alpha_p^i - \alpha_g^i) \times W_\alpha^i)^2}{\sum_i W_\alpha^i}. \quad (4)$$

**Cross Entropy loss** For those methods that involve classification prediction for intermediate representations [27], [34], [37] or refinement of the auxiliary input during training [2], [4], [49], the cross-entropy loss function is often used. The predicted probability for the  $c$ -th class of the intermediate representation is denoted as  $I_p^c \in [0, 1]$ , while the ground truth label is represented by  $I_g^c \in \{0, 1\}$ . The cross-entropy loss function is defined as follows:

$$\mathcal{L}_{ce} = - \sum_{c=1}^C I_g^c \log(I_p^c). \quad (5)$$

**Laplacian loss** The Laplacian loss function is first introduced in Context-aware [32], which is motivated by the work [157] and is defined as the absolute difference between two Laplacian pyramid representations. This loss function can capture local and global differences, as shown in Eq. (6). Here,  $Lap^k(\alpha_g^i)$  and  $Lap^k(\alpha_p^i)$  denote the  $k^{th}$  level Laplacian pyramid of the ground truth alpha map and its prediction, respectively. The contribution of each Laplacian level to the loss is scaled based on its spatial size.

$$\mathcal{L}_{lap} = \sum_i W^i \sum_{k=1}^5 2^{k-1} \left\| Lap^k(\alpha_p^i) - Lap^k(\alpha_g^i) \right\|_1. \quad (6)$$

**Gradient loss** As mentioned in previous studies [11], [90], the above loss functions cannot adequately promote sharpness in the final output, resulting in blurred boundaries. To address this issue, Tang et al. [33] propose a gradient loss that calculates the  $L^1$  distance between the gradient magnitudes of the ground truth and predicted alpha mattes, as shown in Eq. (7). The weight  $W_\alpha^i$  is set as before.

$$\mathcal{L}_{grad} = \frac{\sum_i W_\alpha^i \left\| \nabla \alpha_p^i - \nabla \alpha_g^i \right\|_1}{\sum_i W_\alpha^i}. \quad (7)$$

**Adversarial loss** To improve the quality of the generated composite images, some methods utilize adversarial losses [158]. These methods incorporate a discriminator to differentiate between the predicted composite image and real images. The adversarial loss function is defined as shown in Eq. (8), where  $x$  is a real image,  $D$  is the discriminator, and  $Comp(G(x))$  is a composition function that takes the predicted alpha from the generator  $G$  as input to generate a fake image.

$$\mathcal{L}_{adv} = \log D(x) + \log(1 - D(Comp(G(x)))). \quad (8)$$

**Multi-task loss** Several works, such as the one proposed by Cai et al. [34], employ a multi-stream architecture to perform different sub-tasks, and thus adopt a multi-task loss to supervise the model training. Following the approach suggested by Kendall et al. [159], these works define a loss function that combines different losses for each task. Specifically, the loss function, as shown in Eq. (9), consists of two terms, namely  $\mathcal{L}_{Inter}$  and  $\mathcal{L}_{alpha}$ , which correspond to the loss associated with the intermediate prediction and alpha prediction, respectively. Here,  $\sigma_1$  and  $\sigma_2$  are learnable weights to balance the two sub-tasks.

$$\mathcal{L}_{multi} = \frac{1}{2\sigma_1^2} \mathcal{L}_{Inter} + \frac{1}{\sigma_2} \mathcal{L}_{alpha} + \log 2\sigma_1\sigma_2. \quad (9)$$

**SSIM loss** To enhance the predicted foreground structure, some studies [48] employ the Structural Similarity (SSIM) loss [160], inspired by previous works [146], [161], to improve the consistency of structure in the ground truth and predicted alpha mattes. Eq. (10) demonstrates the SSIM loss, where  $\mu_p$ ,  $\mu_g$ ,  $\sigma_p$ , and  $\sigma_g$  represent the mean and standard deviation of  $\alpha_p$  and  $\alpha_g$ , respectively.

$$\mathcal{L}_{ssim} = 1 - \frac{(2\mu_p\mu_g + c_1)(2\sigma_{pg} + c_2)}{(\mu_p^2 + \mu_g^2 + c_1)(\sigma_p^2 + \sigma_g^2 + c_2)}. \quad (10)$$

## 6.2 Evaluation Metrics

To quantitatively evaluate the quality of predicted results, previous researchers have proposed many evaluation metrics that measure prediction errors from different perspectives. We discuss some of these metrics as follows.

**SAD** SAD is a widely used evaluation metric in the image matting task. It measures the dissimilarity between the predicted alpha matte and the ground truth alpha matte by computing the absolute difference between each pixel and summing up all the values.

**SAD-T** Furthermore, in the context of automatic image matting, researchers have also introduced SAD-T (SAD in transition areas) [4], which is a modified version of SAD that specifically measures the errors in the transition areas, which are known to contain fine details that are crucial for accurate alpha matte prediction.

**MSE** MSE measures the average squared difference between the predicted alpha matte and the ground truth.

**MAD** To address the limitations of SAD and MSE in not accounting for image size and being unsuitable for cross-dataset comparisons, researchers have proposed using MAD (*a.k.a.*, mean absolute difference) [4] as an additional metric for evaluating the quality of predicted alpha mattes.

TABLE 4  
Quantitative results of traditional, auxiliary input-based, and automatic matting methods on four representative matting datasets.

	Method	Pub.	Model Complexity				DIM-481 [22]				alphamating.com [54]			
			Backbone	#Params (M)	Complexity (GMac)	Speed (s) 512 × 512	SAD	MSE	GRAD	CONN	SAD	MSE	GRAD	CONN
Traditional	Bayesian [17]	CVPR'01				20.0852	-	-	-	-	25.61	2.85	2.48	6.34
	ClosedForm [12]	TPAMI'06				1.8197	168.1	0.091	126.9	167.9	17.73	1.62	1.5	0.54
	Robust [8]	CVPR'07				8.7748	-	-	-	-	17.59	1.48	1.2	2.09
	Learning [162]	ICCV'09				3.1127	113.9	0.048	91.6	122.2	17.3	1.44	1.35	1.66
	Shared [163]	CGF'10				98.3686	128.9	0.091	126.5	135.3	13.55	0.88	0.9	0.81
	Global [164]	CVPR'11				3.5040	133.6	0.068	97.6	133.3	12.83	0.81	1.03	1.34
	Comprehensive [19]	CVPR'13				41.4687	143.8	0.071	102.2	142.7	12.73	0.75	0.9	1.21
	KNN [58]	TPAMI'13				6.6741	175.4	0.103	124.1	176.4	12.69	0.7	1.03	0.81
	IFM [11]	CVPR'17				15.8284	75.4	0.066	63.0	-	9.51	0.49	0.78	0.71
Auxiliary	DCNN [21]	ECCV'16	-	1.51	8.74	0.0017	161.4	0.087	115.1	161.9	10.2	0.55	0.79	0.93
	DIM [22]	CVPR'17	VGG-16 [126]	130.55	25.58	0.0440	50.4	0.0014	31.0	50.8	9.64	0.57	0.85	0.73
	AlphaGAN [90]	BMVC'18	ResNet-50 [127]	40.3	203.31	0.0364	52.4	0.0030	38.0	-	10.2	0.55	0.79	0.93
	SampleNet [33]	CVPR'19	-	47.83	392.08	0.2454	40.4	0.0099	-	-	9.47	0.54	0.78	0.89
	AdaMatting [34]	ICCV'19	ResNet-50	8.49	55.85	0.0367	41.7	0.0010	16.8	-	9.06	0.5	0.7	0.55
	IndexNet [24]	ICCV'19	MobileNetV2 [134]	3.18	22.92	0.0142	45.8	0.0013	25.9	43.7	10.31	0.62	0.83	0.69
	Context [32]	ICCV'19	Xception 65 [165]	184.95	205.47	0.0406	35.8	0.0082	17.3	33.2	9.79	0.46	0.64	0.74
	GCA [23]	AAAI'20	ResNet-34 [127]	25.16	0.52	0.0301	35.3	0.0091	16.9	32.5	9.59	0.54	0.66	0.56
	FBA [25]	ArXiv'20	ResNet-50	34.69	7.15	0.0425	25.8	0.0052	10.6	20.8	-	-	-	-
	FDMatting [102]	WACV'21	ResNet-34	29.0	779.43	0.0512	37.6	0.0090	18.3	35.4	-	-	-	-
	HDMatt [96]	AAAI'21	ResNet-34	53.01	1306.06	0.0724	33.5	0.0073	14.5	29.9	8.8	0.41	0.56	0.69
	SIM [95]	CVPR'21	ResNet-50	46.45	19.88	0.0543	28.0	0.0058	10.8	24.8	8.01	0.4	0.49	0.51
	MGMatting [29]	CVPR'21	ResNet-50	29.6	4.37	0.0170	28.9	0.0057	11.4	24.9	-	-	-	-
	TIMI-Net [26]	ICCV'21	ResNet-18 [127]	34.89	3.37	0.0199	29.1	0.0060	11.5	25.4	7.34	0.34	0.45	0.5
	LFPNet [104]	MM'21	ResNet-50	117.61	24.44	0.1084	22.4	0.0036	7.6	17.1	7.67	0.34	0.4	0.5
	FGI [92]	BMVC'21	ResNet-34	26.04	2.35	0.0148	30.19	0.0061	13.07	26.66	9.12	0.47	0.55	0.98
MatteFormer [42]	CVPR'22	Swin [40]	44.75	29.14	0.0545	23.8	0.0040	8.7	18.9	-	-	-	-	
Model Complexity							AM-2K [4]				P3M-10K (P3M-500-NP) [47]			
Automatic	Method	Pub.	Backbone	#Params (M)	Complexity (GMac)	Speed (s) 512 × 512	SAD	MSE	MAD	SAD-T	SAD	MSE	MAD	SAD-T
	SHM [2]	MM'18	ResNet-50	79.27	870.16	0.0993	17.81	0.0068	0.0102	10.26	20.77	0.0093	0.0122	9.14
	LF [49]	CVPR'19	DenseNet-201 [138]	37.91	2821.14	0.1103	36.12	0.0116	0.0210	19.68	32.59	0.0131	0.0188	14.53
	HATT [48]	CVPR'20	ResNeXt-101 [133]	106.96	1502.46	0.0862	28.01	0.0055	0.0161	13.36	30.53	0.0072	0.0176	13.48
	SHMC [45]	CVPR'20	ResNet-34	78.23	139.55	0.0125	61.50	0.0270	0.0356	35.23	31.07	0.0094	0.0179	18.86
	AIM [5]	IJCAI'21	ResNet-34	55.30	99.56	0.0165	13.97	0.0050	0.0081	10.44	13.01	0.0045	0.0075	9.24
	P3M [47]	MM'21	ResNet-34	39.48	80.1	0.0127	13.59	0.0046	0.0078	10.55	11.23	0.0035	0.0065	7.65
	GFM [4]	IJCV'22	ResNet-34	55.29	75.39	0.0135	10.89	0.0029	0.0064	9.15	15.50	0.0056	0.0091	10.16
	MODNet [46]	AAAI'22	MobileNetV2	6.49	20.0	0.0131	19.88	0.0052	0.0116	14.89	15.56	0.0043	0.0090	9.40
	P3M-ViTAE [3]	IJCV'23	ViTAE [52]	27.46	112.01	0.0399	9.75	0.0026	0.0057	8.58	7.59	0.0019	0.0044	6.60

**GRAD** While the aforementioned metrics provide a useful foundation for comparison, they are not always indicative of the visual quality as perceived by human observers. Therefore, some researchers [54] have proposed using gradient errors to measure the difference between the gradients of the predicted alpha matte and the ground truth matte. The gradient is obtained by convolving the alpha mattes with first-order Gaussian derivative filters with a variance.

**CONN** Motivated by previous works [166], [167], researchers [54] propose the CONN metric, which is similar to GRAD and aims to measure the quality of alpha mattes based on the connectivity between the foreground and background regions. Specifically, it defines the degree of connectedness based on the connectivity in binary threshold images computed from the grayscale alpha matte.

### 6.3 Results and Analysis

In this section, we conduct a comprehensive performance evaluation of existing image matting techniques. Specifically, we benchmark both auxiliary input-based methods

and automatic methods. However, the experiment settings vary considerably due to the distinct nature of these two kinds of methods. To this end, we provide a detailed discussion of data augmentation strategies, as well as training and testing protocols. Furthermore, we present both the quantitative and qualitative evaluation results of several representative methods on four public matting datasets, as shown in Table 4, Figure 5, and Figure 6.

#### 6.3.1 Auxiliary Input-based Image Matting

To compare the efficacy of deep learning-based methods against traditional methods, we evaluate their performances on two widely adopted datasets: DIM-481 [22] and alphamating.com [54] and focus on the trimap auxiliary input. Specifically, the results obtained from alphamating.com are reported as the average scores of the prediction results based on the user-defined trimap.

**Data augmentation** As a common practice, the training images are typically subject to random cropping centered on pixels in the transition area [22], and sampled at different sizes (e.g.,  $320 \times 320$ ,  $480 \times 480$ ,  $640 \times 640$ ) before being

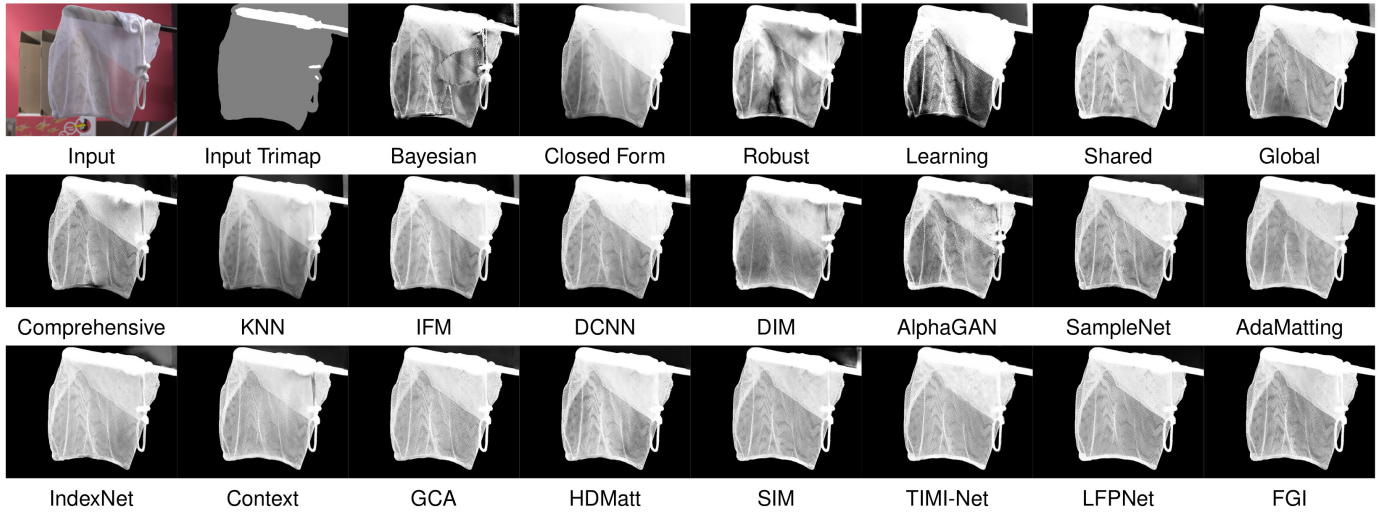


Fig. 5. Some subjective results of auxiliary-based matting methods on alphasamting.com [54]. We suggest enlarging the image for a more detailed view.

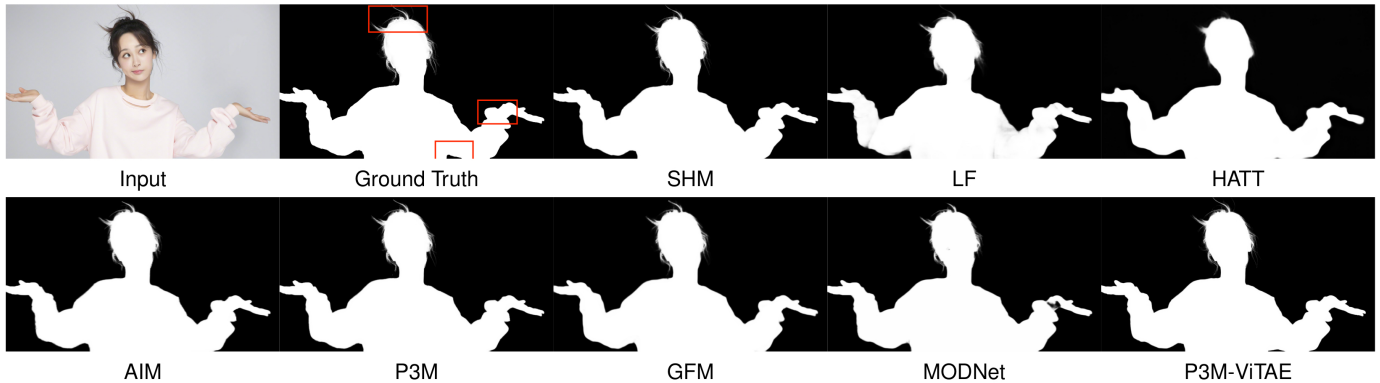


Fig. 6. Some subjective results of automatic matting methods on P3M-500-NP [47]. We suggest enlarging the image for a more detailed view.

resized to  $320 \times 320$  to enhance the robustness of the trained models against variations in scale [22]. Some researchers [33] have extended these strategies by using two foregrounds for composition and randomly changing the brightness, contrast, and saturation. For background image sources, MS COCO [56] and Pascal VOC [57] are commonly adopted. Recently, the use of BG-20K [4] has shown great advantages in terms of diversity, resolution, and quality.

As shown in the top part of Table 4, the results demonstrate a significant performance gap between deep learning-based methods and traditional methods, which is consistent with the subjective results in Figure 5. This can be attributed to the superior representation abilities of deep neural networks, resulting in substantial reductions in SAD from 175.4 to 22.4 on DIM-481 and 25.61 to 7.34 on alphasamting.com. The visual results in Figure 5 also demonstrate the superiority of deep learning-based methods over traditional ones.

Furthermore, the results of deep learning methods reveal some interesting findings. Firstly, transformer-based models exhibit promising potential in predicting fine details, as demonstrated by their performance on DIM-481 [22]. MatteFormer [42], for instance, is a notable example that owes its success to the powerful capacity of capturing global context information. Secondly, multi-stream architectures

that learn the long-range context features together with image patch details have also shown good results, *e.g.*, TIMI-Net [110] on alphasamting.com and LFPNet [104] on DIM-481 [22]. Thirdly, it is also important to note that using only one benchmark may result in bias since the methods may overfit a specific dataset. Hence, it is highly recommended to evaluate the performance of matting methods on various benchmarks. Finally, although the current state-of-the-art deep learning-based matting methods are already demonstrating remarkable potential, there is still room for further studies, such as improving the details of transition areas.

### 6.3.2 Automatic Image Matting

To evaluate the performance of automatic image matting methods, we choose to benchmark them on real-world public datasets, namely AM-2K [4] and P3M-10K [47], to mitigate potential issues arising from resolution discrepancies and semantic ambiguities in composite images [4]. We trained the representative models according to the settings outlined in their respective papers, and in cases where code is unavailable, we re-implement it. All models were trained using the same data augmentation strategies on two NVIDIA Tesla V100 GPUs for a fair comparison.

**Data augmentation** In contrast to trimap-based matting methods, the training images for automatic matting methods are typically cropped and sampled from the entire image instead of only focusing on the transition areas. We adopt augmentation strategies such as Gaussian noise, blur, and sharpness, as suggested by prior studies [4]. Additionally, brightness, color-jitter, flip, and rotation are also employed to enhance the models' generalization abilities.

In the bottom part of Table 4, we report the results of representative automatic matting methods in terms of SAD, MSE, MAD, and SAD-T. These results provide valuable insights into the effectiveness of these methods and future research directions. Firstly, it is found that methods utilizing the encoder-sharing architecture tend to produce favorable results on both datasets, *e.g.*, GFM [4], AIM [5], and P3M [47], highlighting the advantages of decomposing the matting problem into sub-tasks and addressing them jointly. Secondly, the transformer-based model such as P3M-ViTAE [3], has shown superior performance due to its remarkable ability to model long-range dependencies and extract global semantic features. Thirdly, it is noteworthy that the SAD-T metric, which measures the SAD error within the transition area, still accounts for a significant portion of the overall SAD error. This emphasizes the need for future work to focus on reducing errors in transition areas, which often contain many fine details.

## 6.4 Model Complexity Analysis

To provide a comprehensive analysis of the computational complexity and inference speed of various matting methods, we conduct evaluations on a workstation equipped with an Intel Xeon CPU (2.30GHz) and a Tesla V100 GPU. For each method, we record the average inference speed of processing a  $512 \times 512$  image over 100 runs. As can be seen from Table 4, the number of parameters ranges from 3.18M to 184.95M, with complexities varying from 0.52 GMac to 2821.14 GMac, and test speeds ranging from 0.0017 seconds to 0.2454 seconds. Notably, most auxiliary input-based matting methods and automatic matting methods can achieve real-time inference speeds. Nevertheless, there is room for further research to develop more lightweight models while maintaining good performance and fast inference speed.

## 7 APPLICATIONS

Image matting, as a fundamental low-level image processing technique, has enabled the advancement of numerous downstream applications. These applications span a wide range, including e-commerce advertising promotion, image editing for daily entertainment, and virtual reality and augmented reality. In this section, we discuss the applications and research areas that are closely related to image matting by reviewing relevant literature.

**Visual perception** Image matting finds applications in various visual perception tasks such as object detection [168], [169], semantic segmentation [170], [171], [172], [173], obstruction removal [174], and certain specific matting tasks such as cloud matting [175], medical matting [176], and light-field matting [177]. More specifically, image matting is used to refine binary shadow masks [169] after detection,

to learn to predict cloud reflectance and attenuation [175], and to estimate consistent mattes across light-field images based on depth and color [177].

**Image editing** Image matting has also found widespread use in downstream image editing applications such as image composition [66], [178], image inpainting/outpainting [179], [180], image enhancement [181], [182], and image style transfer [183]. Among these, image matting is often used as a common approach for image composition [178], and generates alpha matte and foreground for image relighting [181].

**Video processing** Image matting has also been utilized in various video-related applications, including video effects association [184], shallow depth-of-field synthesis [185], video style transfer [186], multi-view stereo [187], RGB-D matting [188], and video matting [189], [190]. In particular, image matting contributes to generating the training data for shallow depth-of-field synthesis [185], and extracts better portrait foreground with the aid of depth maps [188].

**Multi-modality and 3D applications** Image matting is also used in various multi-modality and 3D applications, such as remote sensing [191], [192], 3D rendering [193], and 3D matting [194]. For instance, researchers have utilized image matting for foreground extraction before 3D rendering [193]. Additionally, they have customized advanced matting algorithms for CT images, allowing for the calibration of the alpha matte with radiodensity [194]. In remote sensing, a deep learning-based matting framework with a clear physical significance is used to detect clouds from remote sensing images [191] and image matting has also been applied to process the intensity component obtained by averaging over each band of multispectral images [192].

In addition to the aforementioned applications, image matting is also being applied in various industrial and entertainment domains. For instance, it is utilized in e-commerce advertisement promotions, automatic driving scene analyses, portrait image editing, and ID photo generation from natural images. Moreover, image matting plays an important role in the metaverse and game industry, where it is used as a pre-processing technique to enable fancy effects and make the rendering process realistic and efficient.

## 8 CHALLENGES AND OPPORTUNITIES

In recent years, image matting has undergone rapid development with the integration of deep learning techniques. Researchers have made significant contributions by proposing new tasks, designing innovative models, improving the optimization process, and establishing large-scale datasets to advance the field. Promising results have been achieved, and some models are even capable of real-time implementation. However, there are still several challenges to overcome and opportunities to explore in this field. In the following section, we discuss the current challenges and highlight potential research directions.

### 8.1 Challenges

**Comprehensive datasets** Establishing a challenging and large-scale dataset is crucial for developing deep learning-based image matting methods. Although researchers have

constructed various training and testing datasets for image matting, these datasets are often biased towards a single category such as humans, animals, or transparent objects [1], [4], [94], suffer from composite artifacts due to the lack of natural images [22], [26], [95], and are not publicly available [2], [45], [109]. Therefore, it is essential to construct more challenging and comprehensive datasets that contain large-scale high-resolution natural images, foregrounds from multiple categories with fine details, diverse backgrounds, and precise high-quality alpha matte annotations.

**Evaluation metrics** Although previous researchers have designed various metrics, such as SAD and MSE, that are capable of evaluating the quality of the predicted alpha mattes in terms of their similarity with the ground truth, there may still exist discrepancies between these evaluation results and the quality perceived by humans [195]. For example, a predicted alpha matte may exhibit a small value of SAD even in the transition regions, yet fail to accurately predict fine details that are important to human observers, such as hair, earrings, or glasses frames. To address this issue, one possible solution is to adopt structural similarity-based metrics, such as SSIM, which prioritize the preservation of fine details. Nevertheless, developing new evaluation metrics that consider the characteristics of the human visual system and are suitable for image matting tasks represents a significant challenge and deserves further research efforts.

**Generalization ability** The generalization ability of current image matting methods is significantly influenced by the training datasets. Models trained on synthetic images have been found to perform poorly on natural images [48], [49], even trained with proper augmentation strategies [4], [32], [43]. Similarly, models trained on single-category images are unable to handle other categories of images [29], [47], [93]. To overcome these limitations, it is necessary to construct more comprehensive datasets and develop advanced training methods that can improve the generalization abilities of image matting models.

**Lightweight model** Since image matting is typically employed in real-time industrial scenarios, advanced architecture designs are required to develop lightweight and computationally efficient models. Some effective ideas such as dimension reduction [127], [134], feature reuse [138], token pruning [196], and hybrid-resolution structure [91], [96] in related areas could be explored for efficient matting.

## 8.2 Future Prospects

**Weakly supervised or unsupervised learning** As the manual effort required to label high-quality matting datasets is significant, there is considerable interest in exploring training data with weak or even no annotations [197], [198], *e.g.*, coarse masks in segmentation dataset [199] and saliency maps in saliency detection datasets [103], [200]. By using them as the pre-training data and transferring the learned knowledge obtained from these tasks to the image matting task, the matting models can obtain good weight initialization and have better generalization abilities [5], [201]. In addition, off-the-shelf deep learning models designed for object detection and semantic segmentation can be leveraged to process unlabeled data and obtain object bounding boxes and masks as weak labels. These weak labels can provide valuable supervisory signals to learn semantic features

for image matting models, which holds great promise for further improving their performance. Therefore, continued research in this direction is highly encouraged.

**Bridging the synthetic and real** As previously discussed, synthetic images are of great importance in image matting due to the low cost to produce large-scale training data. Nevertheless, the use of synthetic images for training may lead to limited generalization ability due to the presence of composite artifacts [4]. Therefore, it is imperative to address this issue in future studies by narrowing the domain gap between synthetic and natural images. Some promising approaches to achieve this include utilizing advanced rendering or image generation techniques, developing effective data augmentation strategies, and exploring domain adaptation and generalization methods [202].

**Multi-modality matting** Collaborating image matting with other modalities can extend its usage scenarios in controllable multi-modality image editing tasks. For instance, following the text instruction, RIM [30] could generate the alpha matte of the foreground that matches the text description from a given image. Further research is warranted to investigate image matting with additional modalities, such as language [203], [204], speech, eye gaze [205], or 3D modeling based on the Neural Radiance Fields (NeRF) [206].

**Diffusion model** Recently, the diffusion model [207] has exhibited remarkable potential in generating data, particularly images, that align well with the training data provided. The rapid advancements of large language models and cross-modality pre-training have enabled the diffusion model to comprehend human language instructions and perform image generation and editing from a blank canvas [208], [209]. Now, an open question arises: *What will be the impact of the diffusion model on the future of image matting, e.g., will it be a devastating setback, or will it herald a new era of possibilities?* Despite the uncertainty, we are cautiously optimistic that image matting will continue to play a crucial role in diffusion model-based image generation and editing due to its inherent flexibility, compositionality, and explainability.

## 9 CONCLUSION

This paper presents a comprehensive review of a substantial amount of literature on image matting. We began with an overview of the historical background and traditional techniques and examined deep learning-based methodologies, categorizing them according to the architectural designs of both auxiliary input-based and automatic image matting models. Then, we compared multiple image matting datasets and evaluated the performance of both traditional and deep learning-based image matting methods and their computing efficiency. Furthermore, we discussed the related applications, existing challenges, and future research opportunities. We believe that this study will facilitate readers in navigating this promising field efficiently and provide useful insights for future research endeavors.

## REFERENCES

- [1] Xiaoyong Shen, Xin Tao, Hongyun Gao, Chao Zhou, and Jiaya Jia. Deep automatic portrait matting. In *Proceedings of the European Conference on Computer Vision*, pages 92–107, 2016.

- [2] Quan Chen, Tiezheng Ge, Yanyu Xu, Zhiqiang Zhang, Xinxin Yang, and Kun Gai. Semantic human matting. In *Proceedings of the ACM international conference on Multimedia*, 2018.
- [3] Sihan Ma, Jizhizi Li, Jing Zhang, He Zhang, and Dacheng Tao. Rethinking portrait matting with privacy preserving. *International journal of computer vision*, 2023.
- [4] Jizhizi Li, Jing Zhang, Stephen J Maybank, and Dacheng Tao. Bridging composite and real: towards end-to-end deep image matting. *International Journal of Computer Vision*, 2022.
- [5] Jizhizi Li, Jing Zhang, and Dacheng Tao. Deep automatic natural image matting. In *Proceedings of the International Joint Conference on Artificial Intelligence*, pages 800–806, 2021.
- [6] Walter Beyer. Traveling-matte photography and the blue-screen system: a tutorial paper. *Journal of the SMPTE*, 1965.
- [7] Thomas Porter and Tom Duff. Compositing digital images. In *Proceedings of the annual conference on Computer graphics and interactive techniques*, pages 253–259, 1984.
- [8] Jue Wang and Michael F Cohen. Optimized color sampling for robust matting. In *Proceedings of the IEEE Conference on Computer Vision and Pattern Recognition*, pages 1–8, 2007.
- [9] Jian Sun, Jiaya Jia, Chi-Keung Tang, and Heung-Yeung Shum. Poisson matting. *ACM Transactions on Graphics*, 2004.
- [10] Xuelong Li, Kang Liu, Yongsheng Dong, and Dacheng Tao. Patch alignment manifold matting. *IEEE Transactions on Neural Networks and Learning Systems*, 29:3214–3226, 2018.
- [11] Yagiz Aksoy, Tunc Ozan Aydin, and Marc Pollefeys. Designing effective inter-pixel information flow for natural image matting. In *Proceedings of the IEEE Conference on Computer Vision and Pattern Recognition*, pages 29–37, 2017.
- [12] Anat Levin, Dani Lischinski, and Yair Weiss. A closed-form solution to natural image matting. *IEEE Transactions on Pattern Analysis and Machine Intelligence*, 30:228–242, 2006.
- [13] Yuanjie Zheng, Chandra Kambhampettu, Jingyi Yu, Thomas Bauer, and Karl Steiner. Fuzzymatte: A computationally efficient scheme for interactive matting. In *Proceedings of the IEEE Computer Vision and Pattern Recognition*, pages 1–8, 2008.
- [14] Jue Wang and Michael F Cohen. An iterative optimization approach for unified image segmentation and matting. In *Proceedings of the IEEE International Conference on Computer Vision*, pages 936–943, 2005.
- [15] Xue Bai and Guillermo Sapiro. A geodesic framework for fast interactive image and video segmentation and matting. In *Proceedings of the IEEE International Conference on Computer Vision*, pages 1–8, 2007.
- [16] Alvy Ray Smith and James F Blinn. Blue screen matting. In *Proceedings of the annual conference on Computer graphics and interactive techniques*, pages 259–268, 1996.
- [17] Yung-Yu Chuang, Brian Curless, David H Salesin, and Richard Szeliski. A bayesian approach to digital matting. In *Proceedings of the IEEE Computer Vision and Pattern Recognition*, volume 2, pages II–II, 2001.
- [18] Mark A Ruzon and Carlo Tomasi. Alpha estimation in natural images. In *Proceedings of the IEEE Computer Vision and Pattern Recognition*, pages 18–25, 2000.
- [19] Ehsan Shahrian, Deepu Rajan, Brian Price, and Scott Cohen. Improving image matting using comprehensive sampling sets. In *Proceedings of the IEEE Computer Vision and Pattern Recognition*, pages 636–643, 2013.
- [20] Jing Zhang and Dacheng Tao. Empowering things with intelligence: a survey of the progress, challenges, and opportunities in artificial intelligence of things. *IEEE Internet of Things Journal*, 8(10):7789–7817, 2020.
- [21] Donghyeon Cho, Yu-Wing Tai, and In-So Kweon. Natural image matting using deep convolutional neural networks. In *Proceedings of the European Conference on Computer Vision*, 2016.
- [22] Ning Xu, Brian Price, Scott Cohen, and Thomas Huang. Deep image matting. In *Proceedings of the IEEE Computer Vision and Pattern Recognition*, pages 2970–2979, 2017.
- [23] Yaoyi Li and Hongtao Lu. Natural image matting via guided contextual attention. In *Proceedings of the AAAI Conference on Artificial Intelligence*, volume 34, pages 11450–11457, 2020.
- [24] Hao Lu, Yutong Dai, Chunhua Shen, and Songcen Xu. Indices matter: Learning to index for deep image matting. In *Proceedings of the IEEE International Conference on Computer Vision*, pages 3266–3275, 2019.
- [25] Marco Forte and Francois Piti'e. F, b, alpha matting. *ArXiv*, abs/2003.07711, 2020.
- [26] Yuhao Liu, Jiake Xie, Xiao Shi, Yu Qiao, Yujie Huang, Yong Tang, and Xin Yang. Tripartite information mining and integration for image matting. In *Proceedings of the IEEE International Conference on Computer Vision*, pages 7555–7564, 2021.
- [27] Xin Yang, Y. Qiao, Shaozhe Chen, Shengfeng He, Baocai Yin, Qiang Zhang, Xiaopeng Wei, and Rynson W. H. Lau. Smart scribbles for image matting. *ACM Transactions on Multimedia Computing, Communications, and Applications*, 16:1–21, 2020.
- [28] Soumyadip Sengupta, Vivek Jayaram, Brian Curless, Steven M Seitz, and Ira Kemelmacher-Shlizerman. Background matting: The world is your green screen. In *Proceedings of the IEEE Computer Vision and Pattern Recognition*, pages 2291–2300, 2020.
- [29] Qihang Yu, Jianming Zhang, He Zhang, Yilin Wang, Zhe Lin, Ning Xu, Yutong Bai, and Alan Yuille. Mask guided matting via progressive refinement network. In *Proceedings of the IEEE Computer Vision and Pattern Recognition*, pages 1154–1163, 2021.
- [30] Jizhizi Li, Jing Zhang, and Dacheng Tao. Referring image matting. In *Proceedings of the IEEE Computer Vision and Pattern Recognition*, 2023.
- [31] Yu Wang, Yi Niu, Peiyong Duan, Jianwei Lin, and Yuanjie Zheng. Deep propagation based image matting. In *Proceedings of the International Joint Conference on Artificial Intelligence*, 2018.
- [32] Qiqi Hou and Feng Liu. Context-aware image matting for simultaneous foreground and alpha estimation. In *Proceedings of the IEEE International Conference on Computer Vision*, pages 4130–4139, 2019.
- [33] Jingwei Tang, Yagiz Aksoy, Cengiz Oztireli, Markus Gross, and Tunc Ozan Aydin. Learning-based sampling for natural image matting. In *Proceedings of the IEEE Computer Vision and Pattern Recognition*, pages 3055–3063, 2019.
- [34] Shaofan Cai, Xiaoshuai Zhang, Haoqiang Fan, Haibin Huang, Jiangyu Liu, Jiaming Liu, Jiaying Liu, Jue Wang, and Jian Sun. Disentangled image matting. In *Proceedings of the IEEE International Conference on Computer Vision*, pages 8819–8828, 2019.
- [35] Xin Yang, Ke Xu, Shaozhe Chen, Shengfeng He, Baocai Yin, and Rynson Lau. Active matting. In *Advances in Neural Information Processing Systems*, volume 31, 2018.
- [36] Tianyi Wei, Dongdong Chen, Wenbo Zhou, Jing Liao, Hanqing Zhao, Weiming Zhang, and Nenghai Yu. Improved image matting via real-time user clicks and uncertainty estimation. In *Proceedings of the IEEE Computer Vision and Pattern Recognition*, pages 15374–15383, 2021.
- [37] Henghui Ding, Hui Zhang, Chang Liu, and Xudong Jiang. Deep interactive image matting with feature propagation. *IEEE Transactions on Image Processing*, 31:2421–2432, 2022.
- [38] Ashish Vaswani, Noam Shazeer, Niki Parmar, Jakob Uszkoreit, Llion Jones, Aidan N Gomez, Łukasz Kaiser, and Illia Polosukhin. Attention is all you need. In *Advances in Neural Information Processing Systems*, 2017.
- [39] Alexey Dosovitskiy, Lucas Beyer, Alexander Kolesnikov, Dirk Weissenborn, Xiaohua Zhai, Thomas Unterthiner, Mostafa Dehghani, Matthias Minderer, Georg Heigold, Sylvain Gelly, Jakob Uszkoreit, and Neil Houlsby. An image is worth 16x16 words: Transformers for image recognition at scale. *ArXiv*, abs/2010.11929, 2020.
- [40] Ze Liu, Yutong Lin, Yue Cao, Han Hu, Yixuan Wei, Zheng Zhang, Stephen Lin, and Baining Guo. Swin transformer: Hierarchical vision transformer using shifted windows. In *Proceedings of the IEEE Computer Vision and Pattern Recognition*, 2021.
- [41] Yufei Xu, Qiming Zhang, Jing Zhang, and Dacheng Tao. ViTAE: Vision transformer advanced by exploring intrinsic inductive bias. In *Advances in Neural Information Processing Systems*, 2021.
- [42] GyuTae Park, SungJoon Son, JaeYoung Yoo, SeHo Kim, and Nojun Kwak. Matteformer: Transformer-based image matting via prior-tokens. In *Proceedings of the IEEE Computer Vision and Pattern Recognition*, pages 11696–11706, 2022.
- [43] Yutong Dai, Brian Price, He Zhang, and Chunhua Shen. Boosting robustness of image matting with context assembling and strong data augmentation. In *Proceedings of the IEEE Computer Vision and Pattern Recognition*, pages 11707–11716, 2022.
- [44] Bingke Zhu, Yingying Chen, Jinqiao Wang, Si Liu, Bo Zhang, and Ming Tang. Fast deep matting for portrait animation on mobile phone. In *Proceedings of the ACM international conference on Multimedia*, pages 297–305, 2017.
- [45] Jinlin Liu, Yuan Yao, Wendi Hou, Miaomiao Cui, Xuansong Xie, Changshui Zhang, and Xian-sheng Hua. Boosting semantic



- human matting with coarse annotations. In *Proceedings of the IEEE Computer Vision and Pattern Recognition*, pages 8563–8572, 2020.
- [46] Zhanhan Ke, Jiayu Sun, Kaican Li, Qiong Yan, and Rynson WH Lau. Modnet: Real-time trimap-free portrait matting via objective decomposition. In *Proceedings of the AAAI Conference on Artificial Intelligence*, volume 36, pages 1140–1147, 2022.
- [47] Jizhizi Li, Sihan Ma, Jing Zhang, and Dacheng Tao. Privacy-preserving portrait matting. In *Proceedings of the ACM International Conference on Multimedia*, pages 3501–3509, 2021.
- [48] Yu Qiao, Yuhao Liu, Xin Yang, Dongsheng Zhou, Mingliang Xu, Qiang Zhang, and Xiaopeng Wei. Attention-guided hierarchical structure aggregation for image matting. In *Proceedings of the IEEE Computer Vision and Pattern Recognition*, 2020.
- [49] Yunke Zhang, Lixue Gong, Lubin Fan, Peiran Ren, Qixing Huang, Huijun Bao, and Weiwei Xu. A late fusion cnn for digital matting. In *Proceedings of the IEEE Computer Vision and Pattern Recognition*, pages 7469–7478, 2019.
- [50] Y. Qiao, Yuhao Liu, Qiang Zhu, Xin Yang, Yuxin Wang, Qiang Zhang, and Xiaopeng Wei. Multi-scale information assembly for image matting. *Computer Graphics Forum*, 39, 2020.
- [51] Zijian Yu, Xuhui Li, Huijuan Huang, Wen Zheng, and Li Chen. Cascade image matting with deformable graph refinement. In *Proceedings of the IEEE International Conference on Computer Vision*, pages 7167–7176, 2021.
- [52] Qiming Zhang, Yufei Xu, Jing Zhang, and Dacheng Tao. Vitaev2: Vision transformer advanced by exploring inductive bias for image recognition and beyond. *International Journal of Computer Vision*, pages 1–22, 2023.
- [53] Qiming Zhang, Jing Zhang, Yufei Xu, and Dacheng Tao. Vision transformer with quadrangle attention. *arXiv preprint arXiv:2303.15105*, 2023.
- [54] Christoph Rhemann, Carsten Rother, Jue Wang, Margrit Gelautz, Pushmeet Kohli, and Pamela Rott. A perceptually motivated online benchmark for image matting. In *Proceedings of the IEEE Computer Vision and Pattern Recognition*, pages 1826–1833, 2009.
- [55] Patrick Pérez, Michel Gangnet, and Andrew Blake. Poisson image editing. In *Proceedings of the annual conference on Computer graphics and interactive techniques*, 2003.
- [56] Tsung-Yi Lin, Michael Maire, Serge Belongie, James Hays, Pietro Perona, Deva Ramanan, Piotr Dollár, and C Lawrence Zitnick. Microsoft coco: Common objects in context. In *Proceedings of the European Conference on Computer Vision*, pages 740–755, 2014.
- [57] Mark Everingham, Luc Van Gool, Christopher KI Williams, John Winn, and Andrew Zisserman. The pascal visual object classes (voc) challenge. *International Journal of Computer Vision*, 88(2):303–338, 2010.
- [58] Qifeng Chen, Dingzeyu Li, and Chi-Keung Tang. Knn matting. *IEEE Transactions on Pattern Analysis and Machine Intelligence*, 35(9):2175–2188, 2013.
- [59] Massimo Piccardi. Background subtraction techniques: a review. In *IEEE International Conference on Systems, Man and Cybernetics*, pages 3099–3104, 2004.
- [60] Jue Wang and Michael F. Cohen. Image and video matting: A survey. *Found. Trends Comput. Graph. Vis.*, 3:97–175, 2007.
- [61] Jagruti Boda and Dhatri Pandya. A survey on image matting techniques. In *International Conference on Communication and Signal Processing*, pages 0765–0770. IEEE, 2018.
- [62] Xiaoqiang Li, Jide Li, and Hong Lu. A survey on natural image matting with closed-form solutions. *IEEE Access*, 7:136658–136675, 2019.
- [63] Guilin Yao, Zhijie Zhao, and Shaohui Liu. A comprehensive survey on sampling-based image matting. In *Computer Graphics Forum*, pages 613–628, 2017.
- [64] Guilin Yao. A survey on pre-processing in image matting. *Journal of Computer Science and Technology*, 32:122–138, 2017.
- [65] CR Dhivyaa and S Anbukkarasi. Video matting, watermarking and forensics. In *Computational Intelligence in Image and Video Processing*, pages 245–257. Chapman and Hall/CRC, 2023.
- [66] Li Niu, Wenyan Cong, Liu Liu, Yan Hong, Bo Zhang, Jing Liang, and Liqing Zhang. Making images real again: A comprehensive survey on deep image composition. *ArXiv*, abs/2106.14490, 2021.
- [67] Shervin Minaee, Yuri Boykov, Fatih Murat Porikli, Antonio J. Plaza, Nasser Kehtarnavaz, and Demetri Terzopoulos. Image segmentation using deep learning: A survey. *IEEE Transactions on Pattern Analysis and Machine Intelligence*, 44:3523–3542, 2020.
- [68] Alberto Garcia-Garcia, Sergio Orts-Escolano, Sergiu Oprea, Victor Villena-Martinez, Pablo Martinez-Gonzalez, and Jose Garcia-Rodriguez. A survey on deep learning techniques for image and video semantic segmentation. *Applied Soft Computing*, 2018.
- [69] Fahad Lateef and Yassine Ruichek. Survey on semantic segmentation using deep learning techniques. *Neurocomputing*, 2019.
- [70] Bo Zhao, Jiashi Feng, Xiao Wu, and Shuicheng Yan. A survey on deep learning-based fine-grained object classification and semantic segmentation. *International Journal of Automation and Computing*, 14:119–135, 2017.
- [71] Martin Thoma. A survey of semantic segmentation. *ArXiv*, abs/1602.06541, 2016.
- [72] Ali Borji, Ming-Ming Cheng, Huaizu Jiang, and Jia Li. Salient object detection: A survey. *Computational Visual Media*, 2014.
- [73] Junwei Han, Dingwen Zhang, Gong Cheng, Nian Liu, and Dong Xu. Advanced deep-learning techniques for salient and category-specific object detection: A survey. *IEEE Signal Processing Magazine*, 35:84–100, 2018.
- [74] Wenguan Wang, Qiuxia Lai, H. Fu, Jianbing Shen, and Haibin Ling. Salient object detection in the deep learning era: An in-depth survey. *IEEE Transactions on Pattern Analysis and Machine Intelligence*, 44:3239–3259, 2019.
- [75] Leo Grady, Thomas Schiwietz, Shmuel Aharon, and Rüdiger Westermann. Random walks for interactive alpha-matting. In *Proceedings of VIIP*, volume 2005, pages 423–429. Citeseer, 2005.
- [76] Yu Guan, Wei Chen, Xiao Liang, Zi’ang Ding, and Qunsheng Peng. Easy matting—a stroke based approach for continuous image matting. In *Computer Graphics Forum*, 2006.
- [77] Yung-Yu Chuang, Aseem Agarwala, Brian Curless, David H Salesin, and Richard Szeliski. Video matting of complex scenes. In *Proceedings of the annual conference on Computer graphics and interactive techniques*, pages 243–248, 2002.
- [78] Morgan McGuire, Wojciech Matusik, Hanspeter Pfister, John F Hughes, and Frédo Durand. Defocus video matting. *ACM Transactions on Graphics*, 24(3):567–576, 2005.
- [79] Ydo Wexler, Andrew Fitzgibbon, and Andrew Zisserman. Image-based environment matting. In *Proceedings, Eurographics Workshop on Rendering*, pages 289–299, 2002.
- [80] Douglas E Zongker, Dawn M Werner, Brian Curless, and David H Salesin. Environment matting and compositing. In *Proceedings of the annual conference on Computer graphics and interactive techniques*, pages 205–214, 1999.
- [81] Qi Duan, Jianfei Cai, Jianmin Zheng, and Weisi Lin. Fast environment matting extraction using compressive sensing. In *2011 IEEE International Conference on Multimedia and Expo*, pages 1–6. IEEE, 2011.
- [82] Tai-Pang Wu, Chi-Keung Tang, Michael S Brown, and Heung-Yeung Shum. Natural shadow matting. *ACM Transactions on Graphics*, 26(2):8–es, 2007.
- [83] Yung-Yu Chuang, Dan B. Goldman, Brian Curless, D. Salesin, and Richard Szeliski. Shadow matting and compositing. In *Proceedings of the annual conference on Computer graphics and interactive techniques*, 2003.
- [84] Jue Wang and Michael F Cohen. Simultaneous matting and compositing. In *Proceedings of the IEEE Computer Vision and Pattern Recognition*, pages 1–8. IEEE, 2007.
- [85] Kalyan Sunkavalli, Micah K. Johnson, Wojciech Matusik, and Hanspeter Pfister. Multi-scale image harmonization. In *Proceedings of the annual conference on Computer graphics and interactive techniques*, 2010.
- [86] Alvy Ray Smith. Alpha and the history of digital compositing. Technical report, Citeseer, 1995.
- [87] R. Fielding. *The Technique of Special Effects Cinematography*. Communication arts books. Hastings House, 1974.
- [88] James F Blinn. Compositing. 1. theory. *IEEE Computer Graphics and Applications*, 14(5):83–87, 1994.
- [89] Alvy Ray Smith. Image compositing fundamentals. *Microsoft Corporation*, 5, 1995.
- [90] Sebastian Lutz, Konstantinos Amliantitis, and Aljosa Smolic. AlphaGAN: Generative adversarial networks for natural image matting. In *British Machine Vision Conference*, page 259, 2018.
- [91] Shanchuan Lin, Andrey Ryabtsev, Soumyadip Sengupta, Brian L Curless, Steven M Seitz, and Ira Kemelmacher-Shlizerman. Real-time high-resolution background matting. In *Proceedings of the IEEE Computer Vision and Pattern Recognition*, 2021.
- [92] Hang Cheng, Shugong Xu, Xiufeng Jiang, and Rongrong Wang. Deep image matting with flexible guidance input. In *British Machine Vision Conference*, 2021.

- [93] Guanying Chen, K. Han, and Kwan-Yee Kenneth Wong. Tomnet: Learning transparent object matting from a single image. *Proceedings of the IEEE Computer Vision and Pattern Recognition*, pages 9233–9241, 2018.
- [94] Huanqia Cai, Fanglei Xue, Lele Xu, and Lili Guo. Transmatting: Enhancing transparent objects matting with transformers. In *Proceedings of the European Conference on Computer Vision*, 2022.
- [95] Yanan Sun, Chi-Keung Tang, and Yu-Wing Tai. Semantic image matting. In *Proceedings of the IEEE Computer Vision and Pattern Recognition*, pages 11120–11129, 2021.
- [96] Haichao Yu, Ning Xu, Zilong Huang, Yuqian Zhou, and Humphrey Shi. High-resolution deep image matting. In *Proceedings of the AAAI Conference on Artificial Intelligence*, pages 3217–3224, 2021.
- [97] Yagiz Aksoy, Tae-Hyun Oh, Sylvain Paris, Marc Pollefeys, and Wojciech Matusik. Semantic soft segmentation. *ACM Transactions on Graphics*, 37:1–13, 2018.
- [98] Holger Caesar, Jasper Uijlings, and Vittorio Ferrari. Coco-stuff: Thing and stuff classes in context. In *Proceedings of the IEEE Computer Vision and Pattern Recognition*, pages 1209–1218, 2018.
- [99] Yaoyi Li, Qin Xu, and Hongtao Lu. Hierarchical opacity propagation for image matting. *ArXiv*, abs/2004.03249, 2020.
- [100] supervise.ly. Supervisely person dataset. *supervise.ly*, 2018.
- [101] Yutong Dai, Hao Lu, and Chunhua Shen. Learning affinity-aware upsampling for deep image matting. In *Proceedings of the IEEE Computer Vision and Pattern Recognition*, pages 6841–6850, 2021.
- [102] Chang Liu, Henghui Ding, and Xudong Jiang. Towards enhancing fine-grained details for image matting. *Winter Conference on Applications of Computer Vision*, pages 385–393, 2021.
- [103] Lijun Wang, Huchuan Lu, Yifan Wang, Mengyang Feng, Dong Wang, Baocai Yin, and Xiang Ruan. Learning to detect salient objects with image-level supervision. In *Proceedings of the IEEE Computer Vision and Pattern Recognition*, pages 136–145, 2017.
- [104] Qinglin Liu, Haozhe Xie, Shengping Zhang, Bineng Zhong, and Rongrong Ji. Long-range feature propagating for natural image matting. In *Proceedings of the ACM international conference on Multimedia*, pages 526–534, 2021.
- [105] Bo Xu, Han Huang, Cheng Lu, Ziwen Li, and Yandong Guo. Virtual multi-modality self-supervised foreground matting for human-object interaction. In *Proceedings of the IEEE International Conference on Computer Vision*, pages 438–447, 2021.
- [106] Yijie Zhong, Bo Li, Lv Tang, Hao Tang, and Shouhong Ding. Highly efficient natural image matting. In *British Machine Vision Conference*, 2021.
- [107] Xiaonan Fang, Song-Hai Zhang, Tao Chen, Xian-Chun Wu, Ariel Shamir, and Shimin Hu. User-guided deep human image matting using arbitrary trimaps. *IEEE Transactions on Image Processing*, 31:2040–2052, 2022.
- [108] Yuanjie Zheng, Yunshuai Yang, Tongtong Che, Sujuan Hou, Wenhui Huang, Yue Gao, and Ping Tan. Image matting with deep gaussian process. *IEEE transactions on neural networks and learning systems*, PP, 2022.
- [109] Bo Xu, Jiake Xie, Han Huang, Ziwen Li, Cheng Lu, Yong Tang, and Yandong Guo. Situational perception guided image matting. In *Proceedings of the ACM international conference on Multimedia*, pages 5283–5293, 2022.
- [110] Shashank Tripathi, Siddhartha Chandra, Amit Agrawal, Amrith Tyagi, James M Rehg, and Visesh Chari. Learning to generate synthetic data via compositing. In *Proceedings of the IEEE Computer Vision and Pattern Recognition*, pages 461–470, 2019.
- [111] Yanan Sun, Chi-Keung Tang, and Yu-Wing Tai. Human instance matting via mutual guidance and multi-instance refinement. In *Proceedings of the IEEE Computer Vision and Pattern Recognition*, pages 2647–2656, 2022.
- [112] Y. MISHIMA. Soft edge chroma-key generation based upon hexoctahedral color space. *U.S. Patent 5,355,174*, 1993.
- [113] Anat Levin, Alex Rav-Acha, and Dani Lischinski. Spectral matting. *IEEE Transactions on Pattern Analysis and Machine Intelligence*, 30(10):1699–1712, 2008.
- [114] Jian Sun, Yin Li, Sing Bing Kang, and Heung-Yeung Shum. Flash matting. In *ACM SIGGRAPH*, 2006.
- [115] Neel Joshi, Wojciech Matusik, and Shai Avidan. Natural video matting using camera arrays. *ACM Transactions on Graphics*, 25(3):779–786, 2006.
- [116] Morgan McGuire, Wojciech Matusik, Hanspeter Pfister, John F. Hughes, and Frédo Durand. Defocus video matting. *ACM Transactions on Graphics*, 24:567–576, 2005.
- [117] Changjiang Yang, Ramani Duraiswami, Nail A Gumerov, and Larry Davis. Improved fast gauss transform and efficient kernel density estimation. In *Proceedings of the IEEE International Conference on Computer Vision*, 2003.
- [118] Carsten Rother, Vladimir Kolmogorov, and Andrew Blake. “grab-cut”: interactive foreground extraction using iterated graph cuts. *ACM SIGGRAPH 2004 Papers*, 2004.
- [119] Yair Weiss and William T Freeman. On the optimality of solutions of the max-product belief-propagation algorithm in arbitrary graphs. *IEEE Transactions on Information Theory*, 2001.
- [120] Richard Szeliski. Locally adapted hierarchical basis preconditioning. *ACM Transactions on Graphics*, 2006.
- [121] A. Berman, A. Dadourian, and P. Vlahos. Method for removing from an image the background surrounding a selected object, 2000.
- [122] Kaiming He, Georgia Gkioxari, Piotr Dollár, and Ross B. Girshick. Mask r-cnn. *IEEE Transactions on Pattern Analysis and Machine Intelligence*, 42:386–397, 2017.
- [123] Arie Berman, Paul Vlahos, and Arpag Dadourian. Comprehensive method for removing from an image the background surrounding a selected subject, October 17 2000. US Patent 6,134,345.
- [124] Jonathan Long, Evan Shelhamer, and Trevor Darrell. Fully convolutional networks for semantic segmentation. In *Proceedings of the IEEE Computer Vision and Pattern Recognition*, 2015.
- [125] Olaf Ronneberger, Philipp Fischer, and Thomas Brox. U-net: Convolutional networks for biomedical image segmentation. In *Medical Image Computing and Computer-Assisted Intervention*, 2015.
- [126] Karen Simonyan and Andrew Zisserman. Very deep convolutional networks for large-scale image recognition. *arXiv preprint arXiv:1409.1556*, 2014.
- [127] Kaiming He, Xiangyu Zhang, Shaoqing Ren, and Jian Sun. Deep residual learning for image recognition. In *Proceedings of the IEEE Computer Vision and Pattern Recognition*, pages 770–778, 2016.
- [128] Tero Karras, Samuli Laine, and Timo Aila. A style-based generator architecture for generative adversarial networks. *Proceedings of the IEEE Computer Vision and Pattern Recognition*, 2018.
- [129] Xudong Mao, Qing Li, Haoran Xie, Raymond YK Lau, Zhen Wang, and Stephen Paul Smolley. Least squares generative adversarial networks. In *Proceedings of the IEEE International Conference on Computer Vision*, pages 2794–2802, 2017.
- [130] Sepp Hochreiter and Jürgen Schmidhuber. Long short-term memory. *Neural Computation*, 9:1735–1780, 1997.
- [131] Ronald J. Williams. Simple statistical gradient-following algorithms for connectionist reinforcement learning. *Machine Learning*, 8:229–256, 1992.
- [132] Alec Radford, Jong Wook Kim, Chris Hallacy, Aditya Ramesh, Gabriel Goh, Sandhini Agarwal, Girish Sastry, Amanda Askell, Pamela Mishkin, Jack Clark, Gretchen Krueger, and Ilya Sutskever. Learning transferable visual models from natural language supervision. In *International Conference on Machine Learning*, 2021.
- [133] Saining Xie, Ross B. Girshick, Piotr Dollár, Zhuowen Tu, and Kaiming He. Aggregated residual transformations for deep neural networks. *Proceedings of the IEEE Computer Vision and Pattern Recognition*, 2016.
- [134] Mark Sandler, Andrew Howard, Menglong Zhu, Andrey Zhmoginov, and Liang-Chieh Chen. Mobilenetv2: Inverted residuals and linear bottlenecks. In *Proceedings of the IEEE conference on computer vision and pattern recognition*, pages 4510–4520, 2018.
- [135] Li Zhang, Mohan Chen, Anurag Arnab, Xiangyang Xue, and Philip H. S. Torr. Dynamic graph message passing networks for visual recognition. *IEEE transactions on pattern analysis and machine intelligence*, PP, 2022.
- [136] Changqian Yu, Yifan Liu, Changxin Gao, Chunhua Shen, and Nong Sang. Representative graph neural network. In *European Conference on Computer Vision*, 2020.
- [137] Hengshuang Zhao, Jianping Shi, Xiaojuan Qi, Xiaogang Wang, and Jiaya Jia. Pyramid scene parsing network. *Proceedings of the IEEE Computer Vision and Pattern Recognition*, 2016.
- [138] Gao Huang, Zhuang Liu, Laurens Van Der Maaten, and Kilian Q Weinberger. Densely connected convolutional networks. In *Proceedings of the IEEE Computer Vision and Pattern Recognition*, pages 4700–4708, 2017.
- [139] Liang-Chieh Chen, George Papandreou, Iasonas Kokkinos, Kevin Murphy, and Alan L Yuille. Deeplab: Semantic image segmentation with deep convolutional nets, atrous convolution, and fully

- connected crfs. *IEEE Transactions on Pattern Analysis and Machine Intelligence*, 40(4):834–848, 2017.
- [140] Kaiming He, Jian Sun, and Xiaoou Tang. Guided image filtering. *IEEE Transactions on Pattern Analysis and Machine Intelligence*, 35:1397–1409, 2010.
- [141] Yunpeng Chen, Haoqi Fan, Bing Xu, Zhicheng Yan, Yannis Kalantidis, Marcus Rohrbach, Shuicheng Yan, and Jiashi Feng. Drop an octave: Reducing spatial redundancy in convolutional neural networks with octave convolution. In *Proceedings of the IEEE International Conference on Computer Vision*, pages 3435–3444, 2019.
- [142] Ibraheem Alhashim and Peter Wonka. High quality monocular depth estimation via transfer learning. *ArXiv*, abs/1812.11941, 2018.
- [143] Tiancai Wang, Tong Yang, Martin Danelljan, Fahad Shahbaz Khan, Xiangyu Zhang, and Jian Sun. Learning human-object interaction detection using interaction points. In *Proceedings of the IEEE Computer Vision and Pattern Recognition*, 2020.
- [144] Jian Shi, Yue Dong, Hao Su, and Stella X Yu. Learning non-lambertian object intrinsics across shapenet categories. In *Proceedings of the IEEE Computer Vision and Pattern Recognition*, pages 1685–1694, 2017.
- [145] Jiang-Jiang Liu, Qibin Hou, Ming-Ming Cheng, Jiashi Feng, and Jianmin Jiang. A simple pooling-based design for real-time salient object detection. In *Proceedings of the IEEE Computer Vision and Pattern Recognition*, pages 3917–3926, 2019.
- [146] Xuebin Qin, Zichen Zhang, Chenyang Huang, Chao Gao, Masood Dehghan, and Martin Jagersand. Basnet: Boundary-aware salient object detection. In *Proceedings of the IEEE Conference on Computer Vision and Pattern Recognition*, 2019.
- [147] Ray - the persistence of vision raytracer.
- [148] Tjeerd van der Ploeg, Peter C. Austin, and Ewout Willem Steyberg. Modern modelling techniques are data hungry: a simulation study for predicting dichotomous endpoints. *BMC Medical Research Methodology*, 14, 2014.
- [149] Ehsan Shahrian, Brian L. Price, Scott D. Cohen, and Deepu Rajan. Temporally coherent and spatially accurate video matting. *Computer Graphics Forum*, 33, 2014.
- [150] Adobe Inc. Adobe photoshop.
- [151] Mark Everingham, Luc Van Gool, Christopher K. I. Williams, John M. Winn, and Andrew Zisserman. The pascal visual object classes (voc) challenge. *International Journal of Computer Vision*, 88:303–338, 2010.
- [152] Yochai Blau and Tomer Michaeli. The perception-distortion tradeoff. In *Proceedings of the IEEE Computer Vision and Pattern Recognition*, 2017.
- [153] Ashwin Swaminathan, Min Wu, and K. J. Ray Liu. Digital image forensics via intrinsic fingerprints. *IEEE Transactions on Information Forensics and Security*, 3:101–117, 2008.
- [154] Shaziya Khan and Swati Shripad Kulkarni. Exposing digital image forgeries by illumination color classification. *International Journal of scientific research and management*, 3, 2015.
- [155] Minyoung Huh, Andrew Liu, Andrew Owens, and Alexei A. Efros. Fighting fake news: Image splice detection via learned self-consistency. In *Proceedings of the European Conference on Computer Vision*, 2018.
- [156] Christoph Rhemann, Carsten Rother, Alex Rav-Acha, and Toby Sharp. High resolution matting via interactive trimap segmentation. In *Proceedings of the IEEE Computer Vision and Pattern Recognition*, pages 1–8. IEEE, 2008.
- [157] Simon Niklaus and Feng Liu. Context-aware synthesis for video frame interpolation. In *Proceedings of the IEEE Computer Vision and Pattern Recognition*, pages 1701–1710, 2018.
- [158] Ian Goodfellow, Jean Pouget-Abadie, Mehdi Mirza, Bing Xu, David Warde-Farley, Sherjil Ozair, Aaron Courville, and Yoshua Bengio. Generative adversarial networks. *Communications of the ACM*, 63(11):139–144, 2020.
- [159] Alex Kendall, Yarin Gal, and Roberto Cipolla. Multi-task learning using uncertainty to weigh losses for scene geometry and semantics. In *Proceedings of the IEEE Computer Vision and Pattern Recognition*, pages 7482–7491, 2018.
- [160] Zhou Wang, Alan C Bovik, Hamid R Sheikh, and Eero P Simoncelli. Image quality assessment: from error visibility to structural similarity. *IEEE transactions on image processing*, 2004.
- [161] Renjie Wan, Boxin Shi, Ling-Yu Duan, Ah-Hwee Tan, and Alex C Kot. Crnn: Multi-scale guided concurrent reflection removal network. In *Proceedings of the IEEE Conference on Computer Vision and Pattern Recognition*, pages 4777–4785, 2018.
- [162] Yuanjie Zheng and Chandra Kambhampettu. Learning based digital matting. In *Proceedings of the IEEE International Conference on Computer Vision*, pages 889–896. IEEE, 2009.
- [163] Eduardo SL Gastal and Manuel M Oliveira. Shared sampling for real-time alpha matting. In *Computer Graphics Forum*, volume 29, pages 575–584. Wiley Online Library, 2010.
- [164] Kaiming He, Christoph Rhemann, Carsten Rother, Xiaoou Tang, and Jian Sun. A global sampling method for alpha matting. In *Proceedings of the IEEE International Conference on Computer Vision*, pages 2049–2056, 2011.
- [165] François Chollet. Xception: Deep learning with depthwise separable convolutions. In *Proceedings of the IEEE International Conference on Computer Vision*, pages 1251–1258, 2017.
- [166] Azriel Rosenfeld. On connectivity properties of grayscale pictures. *Pattern recognition*, 16(1):47–50, 1983.
- [167] Luc Vincent and Pierre Soille. Watersheds in digital spaces: an efficient algorithm based on immersion simulations. *IEEE Transactions on Pattern Analysis & Machine Intelligence*, 13(06):583–598, 1991.
- [168] Deng-Ping Fan, Ge-Peng Ji, Ming-Ming Cheng, and Ling Shao. Concealed object detection. *IEEE Transactions on Pattern Analysis and Machine Intelligence*, 44(10):6024–6042, 2021.
- [169] Ruiqi Guo, Qieyun Dai, and Derek Hoiem. Paired regions for shadow detection and removal. *IEEE Transactions on Pattern Analysis and Machine Intelligence*, 35(12):2956–2967, 2012.
- [170] Naofumi Akimoto, Huachun Zhu, Yanghua Jin, and Yoshimitsu Aoki. Fast soft color segmentation. In *Proceedings of the IEEE Computer Vision and Pattern Recognition*, pages 8277–8286, 2020.
- [171] Di Lin, Jifeng Dai, Jiaya Jia, Kaiming He, and Jian Sun. Scribblesup: Scribble-supervised convolutional networks for semantic segmentation. In *Proceedings of the IEEE Computer Vision and Pattern Recognition*, pages 3159–3167, 2016.
- [172] Swarnendu Ghosh, Nibaran Das, Ishita Das, and Ujjwal Maulik. Understanding deep learning techniques for image segmentation. *ACM Computing Surveys (CSUR)*, 52(4):1–35, 2019.
- [173] Li Gao, Jing Zhang, Lefei Zhang, and Dacheng Tao. Dsp: Dual soft-paste for unsupervised domain adaptive semantic segmentation. In *Proceedings of the ACM international conference on Multimedia*, pages 2825–2833, 2021.
- [174] Yu-Lun Liu, Wei-Sheng Lai, Ming-Hsuan Yang, Yung-Yu Chuang, and Jia-Bin Huang. Learning to see through obstructions. In *Proceedings of the IEEE Computer Vision and Pattern Recognition*, pages 14215–14224, 2020.
- [175] Zhengxia Zou, Wenyuan Li, Tianyang Shi, Zhenwei Shi, and Jieping Ye. Generative adversarial training for weakly supervised cloud matting. In *Proceedings of the IEEE International Conference on Computer Vision*, pages 201–210, 2019.
- [176] Lin Wang, Lie Ju, Donghao Zhang, Xin Wang, Wanji He, Yelin Huang, Zhiwen Yang, Xuan Yao, Xin Zhao, Xiufen Ye, et al. Medical matting: a new perspective on medical segmentation with uncertainty. In *Medical Image Computing and Computer Assisted Intervention*, pages 573–583, 2021.
- [177] Donghyeon Cho, Sunyeong Kim, Yu-Wing Tai, and In So Kweon. Automatic trimap generation and consistent matting for light-field images. *IEEE Transactions on Pattern Analysis and Machine Intelligence*, 39(8):1504–1517, 2016.
- [178] He Zhang, Jianming Zhang, Federico Perazzi, Zhe Lin, and Vishal M Patel. Deep image compositing. In *Winter Conference on Applications of Computer Vision*, pages 365–374, 2021.
- [179] Yanan Zhao, Brian Price, Scott Cohen, and Danna Gurari. Guided image inpainting: Replacing an image region by pulling content from another image. In *Winter Conference on Applications of Computer Vision*, pages 1514–1523. IEEE, 2019.
- [180] Yongzhen Ke, Nan Sheng, Gang Wei, Kai Wang, Fan Qin, and Jing Guo. Subject-aware image outpainting. *Signal, Image and Video Processing*, pages 1–9, 2023.
- [181] Rohit Pandey, Sergio Orts Escolano, Chloe Legendre, Christian Haene, Sofien Bouaziz, Christoph Rhemann, Paul Debevec, and Sean Fanello. Total relighting: learning to relight portraits for background replacement. *ACM Transactions on Graphics*, 40(4):1–21, 2021.
- [182] Yichang Shih, Sylvain Paris, Frédo Durand, and William T Freeman. Data-driven hallucination of different times of day from a single outdoor photo. *ACM Transactions on Graphics*, 2013.
- [183] Fujun Luan, Sylvain Paris, Eli Shechtman, and Kavita Bala. Deep photo style transfer. In *Proceedings of the IEEE Computer Vision and Pattern Recognition*, pages 4990–4998, 2017.

- [184] Erika Lu, Forrester Cole, Tali Dekel, Andrew Zisserman, William T Freeman, and Michael Rubinstein. Omnimatte: associating objects and their effects in video. In *Proceedings of the IEEE Computer Vision and Pattern Recognition*, pages 4507–4515, 2021.
- [185] Lijun Wang, Xiaohui Shen, Jianming Zhang, Oliver Wang, Zhe Lin, Chih-Yao Hsieh, Sarah Kong, and Huchuan Lu. Deeplens: shallow depth of field from a single image. *ACM Transactions on Graphics*, 37(6):1–11, 2018.
- [186] Xide Xia, Tianfan Xue, Wei-sheng Lai, Zheng Sun, Abby Chang, Brian Kulis, and Jiawen Chen. Real-time localized photorealistic video style transfer. In *Winter Conference on Applications of Computer Vision*, pages 1089–1098, 2021.
- [187] Yao Yao, Zixin Luo, Shiwei Li, Tian Fang, and Long Quan. Mvsnet: Depth inference for unstructured multi-view stereo. In *Proceedings of the European Conference on Computer Vision*, pages 767–783, 2018.
- [188] Bo Peng, Mingliang Zhang, Jianjun Lei, Huazhu Fu, Haifeng Shen, and Qingming Huang. Rgb-d human matting: A real-world benchmark dataset and a baseline method. *IEEE Transactions on Circuits and Systems for Video Technology*, 2023.
- [189] Yanan Sun, Guanzhi Wang, Qiao Gu, Chi-Keung Tang, and Yu-Wing Tai. Deep video matting via spatio-temporal alignment and aggregation. In *Proceedings of the IEEE Computer Vision and Pattern Recognition*, pages 6975–6984, 2021.
- [190] Yunke Zhang, Chi Wang, Miaomiao Cui, Peiran Ren, Xuansong Xie, Xian-Sheng Hua, Hujun Bao, Qixing Huang, and Weiwei Xu. Attention-guided temporally coherent video object matting. In *Proceedings of the ACM international conference on Multimedia*, pages 5128–5137, 2021.
- [191] Wenyuan Li, Zhengxia Zou, and Zhenwei Shi. Deep matting for cloud detection in remote sensing images. *IEEE Transactions on Geoscience and Remote Sensing*, 58(12):8490–8502, 2020.
- [192] Yuetao Pan, Danfeng Liu, Liguo Wang, Jón Atli Benediktsson, and Shishuai Xing. Remote sensing image fusion based on nsst and parameter adaptive pcnn. *Journal of Applied Remote Sensing*, 16(4):044519, 2022.
- [193] Erika Lu, Forrester Cole, Tali Dekel, Weidi Xie, Andrew Zisserman, D. Salesin, William T. Freeman, and Michael Rubinstein. Layered neural rendering for retiming people in video. *ACM Transactions on Graphics*, 39:1–14, 2020.
- [194] Lin Wang, Xiufen Ye, Donghao Zhang, Wanji He, Lie Ju, Yi Luo, Huan Luo, Xin Wang, Wei Feng, Kaimin Song, et al. 3d matting: A benchmark study on soft segmentation method for pulmonary nodules applied in computed tomography. *Computers in Biology and Medicine*, 150:106153, 2022.
- [195] Zhou Wang, Alan C Bovik, and Ligang Lu. Why is image quality assessment so difficult? In *2002 IEEE International conference on Acoustics, Speech, and Signal Processing*, volume 4, pages IV–3313. IEEE, 2002.
- [196] Sehoon Kim, Sheng Shen, David Thorsley, Amir Gholami, Woosuk Kwon, Joseph Hassoun, and Kurt Keutzer. Learned token pruning for transformers. In *Proceedings of the 28th ACM SIGKDD Conference on Knowledge Discovery and Data Mining*, pages 784–794, 2022.
- [197] Zhi-Hua Zhou. A brief introduction to weakly supervised learning. *National science review*, 5(1):44–53, 2018.
- [198] Longlong Jing and Yingli Tian. Self-supervised visual feature learning with deep neural networks: A survey. *IEEE Transactions on Pattern Analysis and Machine Intelligence*, pages 4037–4058, 2020.
- [199] Alex Krizhevsky, Ilya Sutskever, and Geoffrey E Hinton. Imagenet classification with deep convolutional neural networks. In *Advances in Neural Information Processing Systems*, 2012.
- [200] Tinglei Feng, Yingjie Zhai, Jufeng Yang, Jie Liang, Deng-Ping Fan, Jing Zhang, Ling Shao, and Dacheng Tao. Ic9600: A benchmark dataset for automatic image complexity assessment. *IEEE Transactions on Pattern Analysis and Machine Intelligence*, 2022.
- [201] Fengxiang He and Dacheng Tao. Super-model ecosystem: A domain-adaptation perspective. *arXiv preprint arXiv:2208.14092*, 2022.
- [202] Qiming Zhang, Jing Zhang, Wei Liu, and Dacheng Tao. Category anchor-guided unsupervised domain adaptation for semantic segmentation. *Advances in Neural Information Processing Systems*, 32, 2019.
- [203] Tingting Qiao, Jing Zhang, Duanqing Xu, and Dacheng Tao. Mirrorgan: Learning text-to-image generation by redescription. In *Proceedings of the IEEE Computer Vision and Pattern Recognition*, pages 1505–1514, 2019.
- [204] Tingting Qiao, Jing Zhang, Duanqing Xu, and Dacheng Tao. Learn, imagine and create: Text-to-image generation from prior knowledge. *Advances in Neural information processing systems*, 2019.
- [205] Carlos H Morimoto and Marcio RM Mimica. Eye gaze tracking techniques for interactive applications. *Computer Vision and Image Understanding*, 98(1):4–24, 2005.
- [206] Ben Mildenhall, Pratul P. Srinivasan, Matthew Tancik, Jonathan T. Barron, Ravi Ramamoorthi, and Ren Ng. Nerf: Representing scenes as neural radiance fields for view synthesis. In *Proceedings of the European Conference on Computer Vision*, 2020.
- [207] Jonathan Ho, Ajay Jain, and Pieter Abbeel. Denoising diffusion probabilistic models. *Advances in Neural Information Processing Systems*, 33:6840–6851, 2020.
- [208] Robin Rombach, Andreas Blattmann, Dominik Lorenz, Patrick Esser, and Björn Ommer. High-resolution image synthesis with latent diffusion models. In *Proceedings of the IEEE Computer Vision and Pattern Recognition*, pages 10684–10695, 2022.
- [209] Bahjat Kawar, Shiran Zada, Oran Lang, Omer Tov, Huiwen Chang, Tali Dekel, Inbar Mosseri, and Michal Irani. Imagic: Text-based real image editing with diffusion models. *arXiv preprint arXiv:2210.09276*, 2022.



**Jizhi Li** received the B.E. degree in electrical engineering from Beihang University and Master's degree in information technology from the University of Melbourne. She is currently pursuing a Ph.D. degree in the School of Computer Science from the University of Sydney. Her research interests include computer vision, image matting, and multi-modal learning. She has published several papers in top-tier conferences and journals including CVPR, IJCV, IJCAI, and Multimedia.



**Jing Zhang** (Member, IEEE) is currently a Research Fellow at the School of Computer Science, The University of Sydney. He has published more than 60 papers in prestigious conferences and journals, such as CVPR, ICCV, ECCV, NeurIPS, ICLR, International Journal of Computer Vision (IJCV), and IEEE Transactions on Pattern Analysis and Machine Intelligence (TPAMI). His research interests include computer vision and deep learning. He is a Senior Program Committee Member of AAAI and IJCAI.



**Dacheng Tao** (Fellow, IEEE) is currently a professor of computer science and an ARC Laureate Fellow in the School of Computer Science and the Faculty of Engineering at The University of Sydney. He mainly applies statistics and mathematics to artificial intelligence and data science. His research is detailed in one monograph and over 200 publications in prestigious journals and proceedings at leading conferences. He received the 2015 Australian Scopus-Eureka Prize, the 2018 IEEE ICDM Research Contributions Award, and the 2021 IEEE Computer Society McCluskey Technical Achievement Award. He is a fellow of the Australian Academy of Science, AAAS, ACM, and IEEE.